ACS OMEGA

Open Access

http://pubs.acs.org/journal/acsodf

Article

New Pathophysiological Insights from Serum Proteome Profiling in Equine Atypical Myopathy

Caroline-J. Kruse,* Marc Dieu, Benoît Renaud, Anne-Christine François, David Stern, Catherine Demazy, Sophie Burteau, François Boemer, Tatiana Art, Patricia Renard, and Dominique-M. Votion

Cite This: https://doi.org/10.1021/acsomega.3c06647

Read Online

ACCESS | Metrics & More | Article Recommendations

ABSTRACT: Equine atypical myopathy (AM) is a severe environmental intoxication linked to the ingestion of protoxins contained in seeds and seedlings of the sycamore maple (*Acer pseudoplatanus*) in Europe. The toxic metabolites cause a frequently fatal rhabdomyolysis syndrome in grazing horses. Since these toxic metabolites can also be present in cograzing horses, it is still unclear as to why, in a similar environmental context, some horses show signs of AM, whereas others remain clinically healthy. Label-free proteomic analyses on the serum of 26 diseased AM, 23 cograzers, and 11 control horses were performed to provide insights into biological processes and pathways. A total of 43 and 44 differentially abundant proteins between "AM vs cograzing horses" and "AM vs control horses" were found. Disease-linked changes in the proteome of different groups were found to correlate with detected amounts of toxins, and principal component analyses were performed to identify the 29 proteins representing a robust AM signature. Among the pathway-specific changes, the glycolysis/gluconeogenesis pathway, the coagulation/complement cascade, and the biosynthesis of amino acids were affected. Sycamore maple poisoning results in a combination of inflammation, oxidative stress, and impaired lipid metabolism, which is trying to be counteracted by enhanced glycolysis.

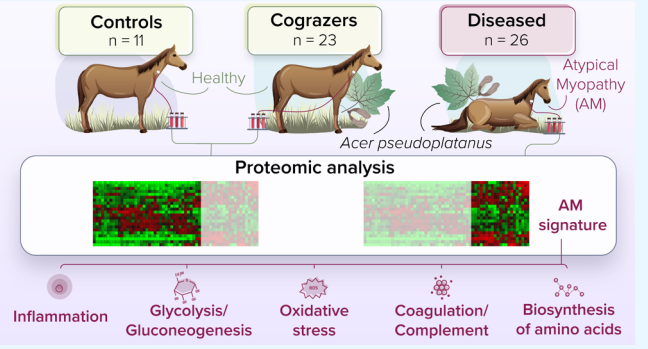

1. INTRODUCTION

Equine atypical myopathy (AM) is a severe environmental poisoning linked to the ingestion of certain maple tree (*Acer*) seeds and seedlings. In Europe, the sycamore maple (*Acer pseudoplatanus*) has been the main species connected to the disease.[1] The intoxication has been associated with two protoxins: hypoglycin A (HGA) and methylenecyclopropylglycine.[2,3] These molecules are not poisonous in themselves but are converted into toxic metabolites, methylenecyclopropylacetyl-CoA (MCPA-CoA) and methylenecyclopropylformyl-CoA (MCPF-CoA), respectively.[4−7] The first step of this conversion in the muscle is the reversible transamination performed by the branched-chain amino acid aminotransferase isoenzymes (BCATm and BCATc).[6,8,9] The second mitochondrial step is irreversible and is performed by the branched-chain α-ketoacid dehydrogenase complex (BCKDHc).[6,8,9] Both active metabolites are fatty-acid β-oxidation inhibitors, resulting in severe energetic impairment in oxidative muscles such as postural, respiratory muscles, and the myocardium.[10−13] Additionally, both interfere with branched-chain amino acid catabolism.[6,14]

The diagnosis of AM results from a combination of compatible clinical signs and strongly increased serum creatine kinase (CK) activity, linked to the severe rhabdomyolysis, the presence of toxic metabolites conjugated with glycine or carnitine, and elevated levels of acylcarnitines.[15] The presence of protoxins in blood is not considered a reliable diagnostic factor as it has previously been published that HGA can be detected in the serum of unaffected cograzing horses.[16] Since toxic metabolites can also be present in cograzing horses,[17,18] it is still unclear as to why, in a similar environmental context, some horses show signs of AM, while others remain clinically healthy. The lethality rate in diseased horses is of 74% that varies between countries and years (ranging from 43[19] to 97%[20]) and, despite extensive research over the past two decades, there is still no cure for intoxicated horses.[21,22]

Since proteomics investigations can help understand the mechanism of toxin-induced damage, it can possibly provide

Received: September 4, 2023
Revised: December 15, 2023
Accepted: December 29, 2023

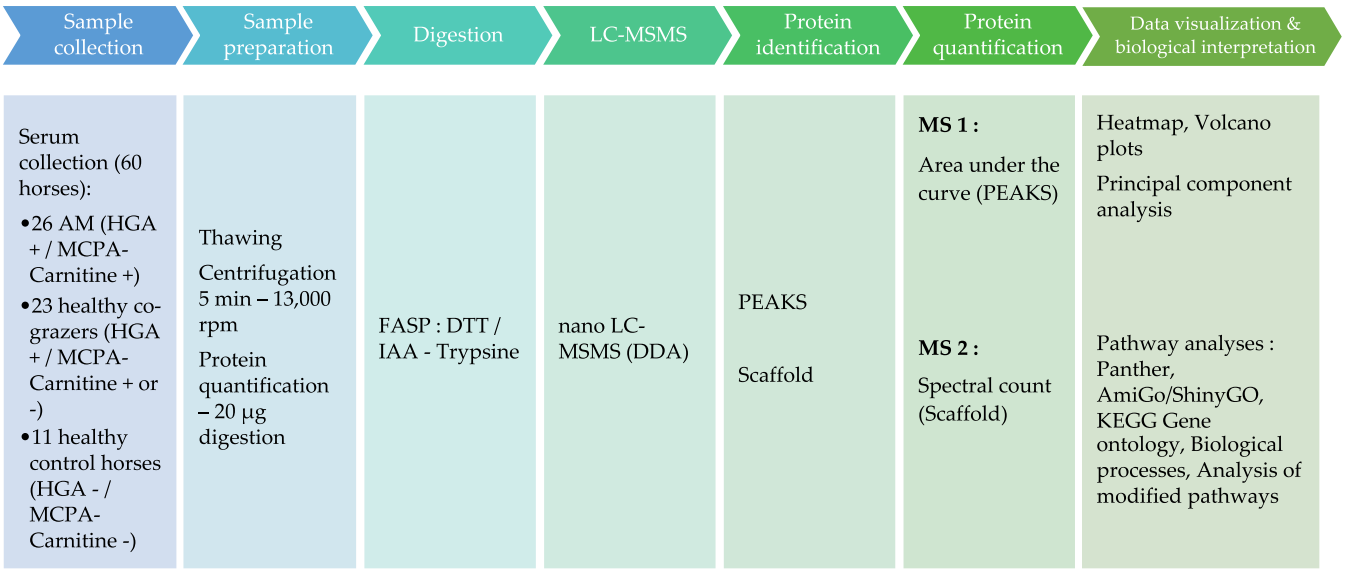

Figure 1. Workflow of sample preparation and proteomic analysis.

new therapeutic approaches.[23,24] Furthermore, proteomics-based technologies provide new insights into potential diagnostic biomarkers, pathogenicity, and the interpretation of functional pathways in diseases.[25]

Using the advantages of the technique, we hypothesized that (1) we would observe disease-linked changes in the proteome of AM-affected horses, (2) that the observed proteomic changes would provide new insights into the disease on the molecular level, and (3) that the amount of detected protoxins and/or toxic metabolites (i.e., HGA/MCPA-carnitine) quantified in the serum is correlated with observed proteomic changes. To identify proteomic signatures responding to toxin exposure, the corresponding genes were aligned to the expressed proteins. Subsequently, the metabolic network was mapped, and enriched pathways were graphically represented. Additionally, biological processes were analyzed through their directionality (over- or under-abundance) to investigate the consequences of the intoxication on horse metabolism.

2. MATERIALS AND METHODS

2.1. Animal Inclusion Criteria and Sampling. Blood samples were collected in the peak months of AM incidences (i.e., in autumn, from October to December and during the following spring from March to May).[26] Sampling took place between 2018 and 2020. The horses were classified into three categories: AM horses, cograzing horses, and control horses, which will be further elaborated upon in this section.

The blood specimens were obtained either as a part of therapeutic procedures initiated by the Equine Veterinary Hospital of the University of Liège (AM horses) or were taken on the field after horse owners provided informed consent for their horses' inclusion in the study (cograzers and control horses). Blood samples collected by jugular venipuncture were extempore kept at 4 °C for a maximum of 2 h before centrifugation and were then stored at −80 °C until further analysis. All procedures adhered to national and international guidelines for animal welfare as the study design is a part of routine veterinary practice to establish a diagnosis or preventing AM. The study also obtained approval from the Animal Ethics Committee of the University of Liège to ensure compliance with ethical standards.

Briefly, every horse with a tentative diagnosis of AM was sampled upon arrival at the equine hospital, preceding any fluid therapy. All included AM horses were considered highly likely to have AM based on the diagnostic algorithm published by van Galen in 2012.[19] These horses exhibited frequent clinical signs of AM, had access to pasture, and showed serum CK activity exceeding 10,000 UI/L and/or pigmenturia.[19] Within 24 h of admission of the suspected AM case, blood samples were taken at pasture from their equine cograzers. Cograzers shared the same pasture as the diseased horses, presented no clinical sign of AM, and underwent a general examination revealing no abnormalities. To be included in the study, cograzers had to have measurable quantities of HGA in their serum, confirming the ingestion of toxins.

Additionally, a group of healthy control horses was also sampled at pasture during the corresponding periods. Control horses had the same duration of pasture exposure as the other two groups, exhibited no clinical abnormalities, and did not show detectable levels of toxins in their blood.

A total of 41 AM horses, 28 cograzing horses, and 19 control horses met the inclusion criteria. A random selection process was employed to designate 26 AM horses, 23 cograzing horses, and 11 control horses from each, respective, category.

To summarize, horses included in this study had to meet different criteria to be included in one of the following three groups: (1) "AM horses", consisting of 26 diseased horses with a highly probable AM diagnosis based on clinical signs, (2) "cograzers", comprising 23 clinically healthy horses cograzing with the diseased horses, and (3) "control horses", consisting of 11 healthy grazing horses in which neither HGA nor MCPA-carnitine was detected.

2.2. HGA Assay. Serum HGA assays were performed according to a previously published technique.[27,28] Quantification of HGA was performed using the aTRAQ kit for amino acid analysis of physiological fluids. HGA contained in samples was derivatized using an isotopic tag (mass m/z = 121), while a second labeling reagent (mass m/z = 113) allowed absolute quantification. Derivatized samples were analyzed through a TQ5500 tandem mass spectrometer (Sciex) using a Prominence AR HPLC system (Shimadzu). The lower limit of quantification associated with this method is 0.090 μmol/L.[27]

https://doi.org/10.1021/acsomega.3c06647
ACS Omega XXXX, XXX, XXX−XXX

2.3. MCPA-Carnitine Determination Method. The MCPA-carnitine separation and determination were carried out by ultraperformance liquid chromatography combined with subsequent mass spectrometry (UPLC−MS/MS). This method has a limit of detection of approximately 0.001 nmol/L.[29]

2.4. Proteomic Workflow. The different steps are illustrated in Figure 1.

2.4.1. Serum Collection and Quantification. Serum samples from a total of 60 horses were collected and subjected to proteomic analysis. The serum samples, which had been stored at −80 °C, were thawed at room temperature and briefly vortexed. The protein concentration of each sample was determined using a Pierce 660 nm protein assay kit (Thermo-Fisher Scientific, USA) following manufacturer's instructions. Subsequently, the samples were divided into aliquots with a concentration of 10 μg/μL.

2.4.2. Protein Digestion. Serum samples were digested using filter-aided sample preparation.[30] First, the Millipore Microcon 30 MRCFOR030 Ultracel PL-30 columns (Merck, Germany) were conditioned using 100 μL of 1% formic acid and centrifuged at 14,500 rpm for 15 min. A centrifugation time of 15 min at 14,500 rpm was used unless otherwise specified. Each sample, containing 20 μg of protein in 100 μL of 8 M urea buffer, was loaded into a column and centrifuged as before. The filtrate was discarded, and the filters were washed three times with urea buffer before centrifugation.

Reduction was performed by adding 100 μL of dithiothreitol (DTT) to the columns, followed by mixing at 400 rpm for 1 min using a thermomixer, and then incubating for 15 min at 24 °C. Subsequent alkylation was achieved by adding 100 μL of iodoacetamide (IAA) to the columns, mixing at 400 rpm for 1 min, and incubating for 20 and 10 min centrifugation at 14,500 rpm. The entire alkylation steps were conducted in the dark before removing the excess of IAA through centrifugation after the addition of urea buffer. To quench the remaining IAA, 100 μL of DTT was added to the columns, mixed at 400 rpm for 1 min, incubated for 15 min at 24 °C, and then centrifuged at 14,500 rpm for 10 min. Excess DTT was removed by adding 100 μL of urea buffer to the column, followed by centrifugation. The column was then washed three times with 100 μL of 50 mM sodium bicarbonate buffer (ABC buffer) and centrifuged for 10 min. The remaining 100 μL was retained in the column to avoid evaporation.

The digestion step was performed by adding 80 μL of mass spectrometry-grade trypsin (Promega, USA) diluted 1/50 in ABC buffer to the column and mixing at 300 rpm for 1 min. The mixture was then incubated overnight at 24 °C. The next day, the Microcon columns were transferred to a LoBind tube of 1.5 mL and centrifuged for 10 min. Subsequently, 40 μL of ABC buffer was added to the column and centrifuged for 10 min. To obtain a 0.2% trifluoroacetic acid (TFA) solution, TFA (10% in ultrapure water) was added to the content of the LoBind tube. The samples were dried using a SpeedVac (Thermo Scientific, USA), resuspended in a solution of 2% acetonitrile and 0.1% formic acid, and transferred to an injection vial.

2.4.3. LC−MS Analysis. Data-dependent LC−MS analyses were performed using a nano-LC−electrospray ionization (ESI)-MS/MS timsTOF Pro (Bruker, Billerica, MA, USA) coupled with a UHPLC nanoElute (Bruker).

Peptides were separated by nanoUHPLC (nanoElute, Bruker) on a 75 μm ID, 25 cm C18 column with an integrated CaptiveSpray insert (Aurora, Ionopticks, Melbourne) at a flow rate of 200 nL/min, at 50 °C. LC mobile phases A was water with 0.1% formic acid (v/v) and B was ACN with 0.1% formic acid 0.1% (v/v). Samples were loaded directly onto the analytical column at a constant pressure of 600 bar. The digest (1 μL) was injected, and the organic content of the mobile phase was increased linearly from 2% B to 15% in 18 min, from 15% B to 25% in 9 min, from 25% B to 37% in 3 min, and from 37% B to 95% in 5 min. Data acquisition on the timsTOF Pro was performed using Hystar 6.0 and timsControl 2.0. timsTOF Pro data were acquired using 160 ms TIMS accumulation time, with mobility ($1/K_0$) ranging from 0.7 to 1.4 Vs/cm^2.

MA analyses were conducted using the parallel accumulation serial fragmentation (PASEF) acquisition method.[31] Each cycle consisted of one MS spectrum, followed by six PASEF MS/MS spectra, with a total cycle time of 1.16 s. Two injections were performed for each sample.

2.4.4. Protein Identification. Tandem mass spectra were extracted and charge state was deconvoluted and deisotoped by Data analysis (Bruker) version 5.3. All MS/MS samples were analyzed using a Mascot (Matrix Science, London, UK; version 2.7). Mascot was set up to search the *Equus caballus* NCBI database (2,177,884 entries) assuming the digestion enzyme trypsin. Mascot was searched with a fragment ion mass tolerance of 0.05 Da and a parent ion tolerance of 15 PPM. Carbamidomethyl of cysteine was specified in Mascot as fixed modifications. Oxidation of methionine and acetylation of the *N*-terminus were specified in Mascot as variable modifications.

Scaffold (version 5.1.0) was used to validate MS/MS-based peptide and protein identifications. Protein identifications were conducted using PEAKS search engine with 15 PPM as parent mass error tolerance and 0.05 Da as fragment mass error tolerance, and protein quantification was based on peptide features detected from LC−MS/MS data by integrating the area under the curve. Peptide identifications were accepted if they could be established at greater than 95.0% probability to achieve an FDR less than 1.0% by the Scaffold Local FDR algorithm. Protein identifications were accepted if they could be established at greater than 5.0% probability to achieve an FDR less than 1.0% and contained at least two identified peptides.

Quantitative analysis was performed using PEAKS Studio X Pro with an ion mobility module and Q module for label-free quantification (Bioinformatics Solutions Inc., Waterloo, ON).

Extensive quality controls were installed. Indeed, in LC−MS-based proteomic studies, performing robust quality control can enhance overall protein quantification and subsequently improve accurate statistical estimates of differential abundance by detecting outlier data points.[32,33] All samples were therefore digested during the same week, and all analyses were conducted with the same LC column to limit variations in peak intensities and identified peptides.[32,33] A control sample (HeLa digest) was injected once in every 10 analyses.

The label-free quantitation method employed in this study utilized an expectation-maximization algorithm applied to the extracted ion chromatograms of the three most abundant unique peptides of a protein, allowing calculation of the area under the curve.[34] Mass error tolerance was set at 15 ppm, and ion mobility tolerance was set at 0.05 $1/K_0$ for quantitation purposes. For label-free quantitation results, the peptide quality score was set to be ≥4, confident number samples per group was ≥5, and the protein significance score threshold was set to 15. The significance score is calculated as the $-10 \log_{10}$ of the significance testing p-value (0.05). Significance testing was performed using ANOVA, excluding modified peptides and

https://doi.org/10.1021/acsomega.3c06647
ACS Omega XXXX, XXX, XXX−XXX

Table 1. Demographic and HGA/MCPA-Carnitine Blood Level Data of Sampled Horses. Age is given in Years, HGA is given in μmol/L, and MCPA-Carnitine in nmol/L[a]

	AGE	HGA (μmol/L)	MCPA-carnitine (nmol/L)
CONTROL HORSES			
MEAN ± SD	11.5 ± 7.6	N/A	N/A
COGRAZING HORSES			
MEAN ± SD	14.5 ± 7.5	1.1 ± 1.1	3.7 ± 7.5
DISEASED HORSES			
MEAN ± SD	6.3 ± 5.2	5.2 ± 5.2	366.5 ± 861.6

[a]Data are presented as means + standard deviation. N/A: not applicable.

requiring at least two peptides for protein quantitation. Normalization factors were calculated by using total ion current.

Two types of statistical analyses were conducted on the identified proteins. First, total spectral counting analysis in Scaffold was performed after identification through Mascot using normalized *t* tests and a Benjamini−Hochberg correction. Second, ion-intensity-based label-free quantitative analysis was performed in PEAKS Studio X Pro after peptide identification by PEAKS.

The biological significance of the confidently identified proteins was determined using the Panther protein classification tool, which evaluated distinct differentially abundant proteins (DAPs) between groups.[35] To visualize the overlaps among enriched pathways and perform direct comparisons across different databases, ShinyGO (version 0.76.1) was utilized, employing clustering techniques. The Kyoto encyclopedia of genes and genomes (KEGG) was employed for mapping of the identified proteins and visualizing metabolic pathways.[36,37] Additional details on the software and analyses performed can be found in the Appendix.

2.4.5. Protein Validation. To validate the findings obtained by LC−MS, we utilized technical replicates of serum samples from 50 horses. Western blotting analysis was performed using the primary antibodies listed in Appendix, secondary antibodies were coupled to infrared dyes [1:10,000 (antimouse or antirabbit IgG), Li-Cor Biosciences, Lincoln, NE, USA], and detection was done by infrared fluorescence (Amersham Typhoon, Cytiva, US). The protein quantification involved establishing a ratio between the protein of interest and the total protein count, which was measured using the No-Stain Protein Labeling Reagent (Thermo Scientific), and normalization across membranes was performed through the pool ratio. To assess significance, *t* tests were employed for data that followed a normal distribution, while Mann−Whitney tests were utilized for non-normally distributed data.

2.5. Statistical Analyses. Raw files were processed with MaxQuant (version 2.1.0.0), searching the *Equus* protein database (*E. caballus* NCBI) supplemented with contaminants. Carbamidomethylation of cysteines, oxidation of methionine, and protein *N*-term acetylation were set as variable modifications. Minimal peptide length was set to seven amino acids, and a maximum of two tryptic missed cleavages were allowed. Results were filtered at 1% false-discovery rate (peptide and protein level), and only proteins with at least two identified peptides were considered for further analysis. To enhance data comparability across different runs, the "match between runs" option was enabled with a match window of 0.7, a match ion mobility window of 0.05, and an alignment window of 20 min. The resulting ".txt" file was then imported into Perseus software (v2.0.7.0) where data filtering was applied to exclude reverse proteins and proteins identified solely by site. The data was then log 2 transformed to convert zero value to "NaN". The resulting matrix was exported and further analyzed using SAS software (version 9.4M7).

Principal component analysis (PCA) was employed to visualize the proteome of individual horses in this study. PCA is a suitable statistical model for this purpose due to the large number of identified proteins. The outcome of PCA is a two-dimensional projection, where each horse is represented as a single point. The *x*-axis (principal component 1) and *y*-axis (principal component 2) are constructed variables derived from linear combinations of the original variables. PCA is an unsupervised method, meaning that it does not consider predefined groups but rather explores the multivariate data set to identify potential group trends. PCAs provide both group discrimination and an overview of the relevant variables. The most influential proteins, which have the strongest impact on the principal components of PCA, were identified and further analyzed.

3. RESULTS

3.1. HGA and MCPA-Carnitine Blood Content. Demographic data for the included horses are provided in Appendix and summarized in Table 1. In control horses, the average age was 11.5 (±7.6) years with a similar distribution of gender (i.e., four geldings, four mares, and three stallions). In cograzing horses, the average age was 14.5 (±7.5) years with 12 geldings, 9 mares, and 2 stallions. Last, we sampled a total of 11 geldings, 8 mares, and 7 stallions in the group of AM horses with an average age of 6.3 (±5.2) years. These age distributions align with previous demographic data, which have reported lower ages in horses with AM compared to clinically healthy horses. So far, there is no gender predisposition reported in relation to AM.[38]

In the group of horses diagnosed with AM, a total of 15 horses either died or were euthanized. Among them, one horse (horse no. 4) was euthanized against medical advice, while 11 horses successfully survived the condition.

Cograzing horses had quantifiable amounts of HGA and in most cases MCPA-carnitine in their blood samples, which proved ingestion of sycamore maple seeds or seedlings. In healthy control horses, neither HGA nor MCPA-carnitine were detected above detection limit.

In diseased animals, the concentrations of HGA ranged from 0.14 to 20 μmol/L, whereas in healthy cograzers, the range was 0.06−4.14 μmol/L. In terms of MCPA-carnitine concentrations, a considerable variation was observed among individuals. In healthy cograzers, the concentrations ranged from 0 to 34.4 nmol/L, while in diseased horses, the concentrations spanned a

https://doi.org/10.1021/acsomega.3c06647
ACS Omega XXXX, XXX, XXX−XXX

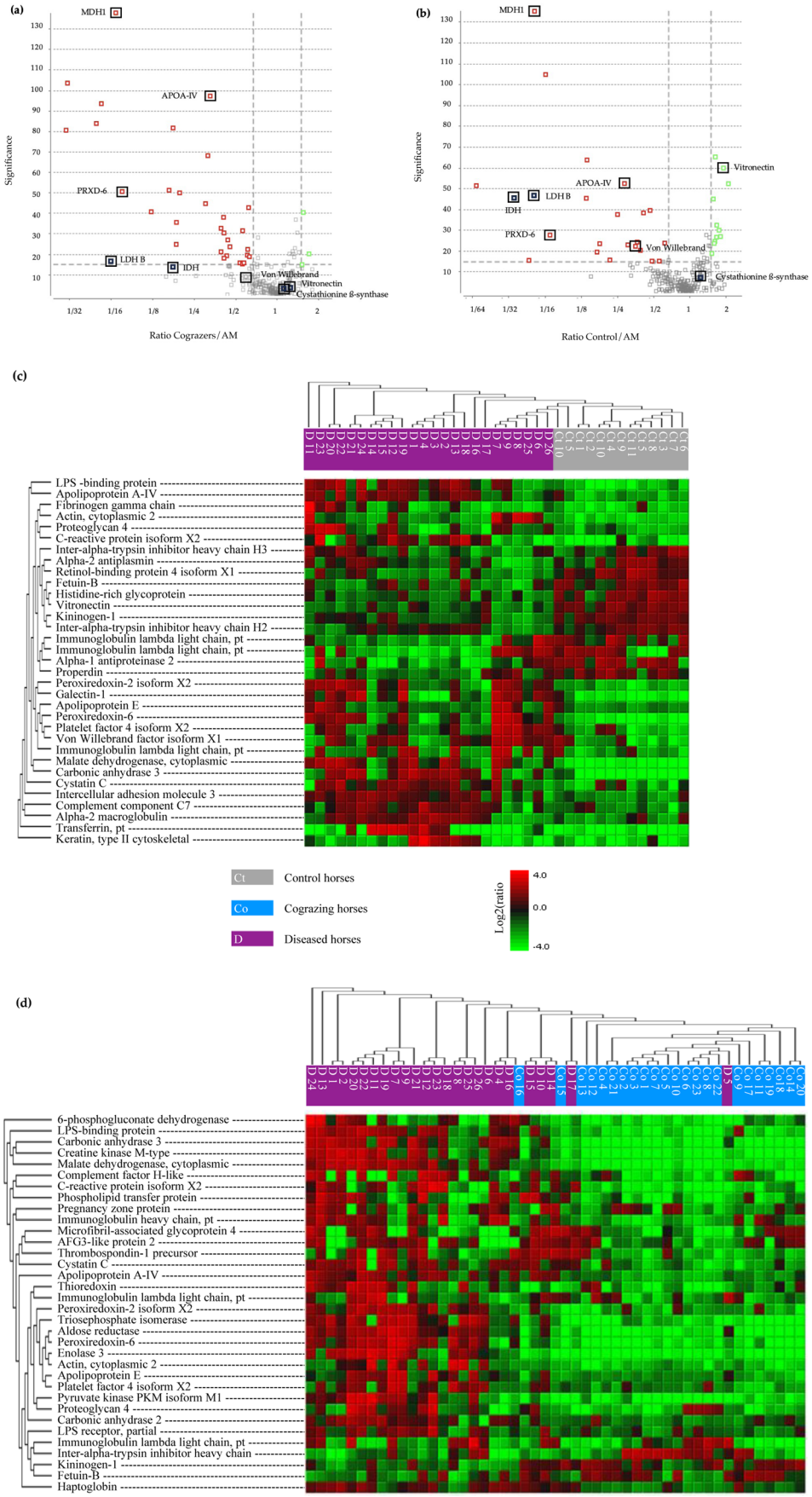

Figure 2. continued

https://doi.org/10.1021/acsomega.3c06647
ACS Omega XXXX, XXX, XXX−XXX

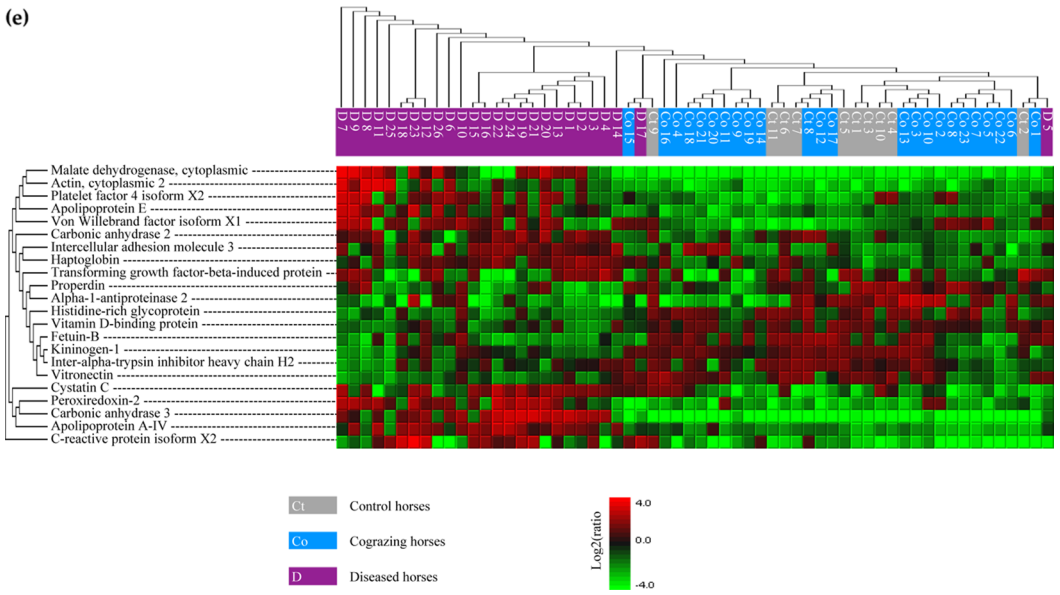

Figure 2. Volcano plots of DAPs (identified through area under the curve analysis) between diseased and healthy cograzing horses (a) and between diseased and control horses (b). On the *x*-axis, the over- and under-abundance thresholds are depicted as vertical gray lines, and their value is set at 1.5. These thresholds help identify proteins that exhibit significant fold changes in abundance between the compared groups. The *y*-axis on these plots represents the chosen significance threshold of 15, which corresponds to a *p*-value of less than 0.05. The significance values are calculated using −10 log(*p*-value) calculations. In summary, the volcano plots provide a visual representation of the DAPs, highlighting those that are statistically significant and have notable fold changes in abundance between the respective, groups of diseased and healthy cograzing horses and between diseased and control horses. The three lines separate the plot into six different regions. Data points that are found in both the top-right and top-left sections of this plot are related to proteins that are statistically significant, beyond the set fold change and significance thresholds. The green squares represent down-regulated proteins, and red squares represent up-regulated proteins in clinically affected AM horses. Proteins labeled on the volcano plot underwent further validation via Western blot analysis. Blue squares denote proteins that did not meet the criteria outlined in the Materials section in PEAKS, either due to identification in fewer than five samples per group or possessing a quality score below 4. (c−e) Heat maps of DAPs (identified through ion mobility analysis) between diseased and healthy cograzing horses (c) and between diseased and control horses (d) and between all three categories simultaneously (e). AM horses are marked by a "D" preceding their identification number, cograzers by a "Co", and control horses by "Ct". Representative proteins (significance ≥15 and fold change ≥1.5) were clustered through expression similarities. A hierarchical clustering was generated by PEAKS using neighbor joining algorithm with a Euclidean distance similarity measurement of the log 2 ratios of the abundance of each sample relative to the average abundance.

wider range of 16.5−4480 nmol/L. It is noteworthy that among the diseased horses, only one horse had a concentration exceeding 1000 nmol/L (specifically, 4480 nmol/L), whereas the mean concentration among the other 25 horses was 202 nmol/L. Additionally, this particular horse also exhibited the highest HGA concentration (20 μmol/L).

3.2. Proteomic Pattern Analysis in "AM Horses" vs "Control Horses" and "AM Horses" vs "Cograzing Horses". *3.2.1. Differentially Abundant Proteins between Groups.* For qualitative analysis, a comprehensive number of 17,462 peptides and 2736 proteins were successfully identified using the Mascot search engine, employing target/decoy strategies. The individual proteins were clustered into 1210 protein families and are presented in Appendix. Notably, the group of horses diagnosed with AM exhibited the highest number of identified proteins among the three groups studied.

To investigate differential abundance patterns, spectral counts were normalized and subjected to *t* tests, followed by a Benjamini−Hochberg correction for multiple testing. Comparative analysis between the AM group and the cograzing group revealed 230 proteins that displayed statistically significant differential abundance. Similarly, a comparison between the AM group and the control group identified 156 proteins with differential protein abundance levels.

Subsequently, the proteome was subjected to quantitative analysis utilizing PEAKS Studio, employing an area under the curve integration. Notably, 43 proteins exhibited differential protein abundance between "AM vs cograzing horses," while 44 proteins displayed differential protein abundance between "AM vs control horses." The volcano plot, illustrated in Figure 2, effectively portrays the proteins that exhibited distinct expression patterns, wherein green and red squares symbolize proteins that were under- and over-abundant in AM horses, respectively. The *x*-axis representing a ratio is determined by dividing the measurement of abundance in clinically healthy horses by the corresponding measurement in diseased horses. It quantifies the magnitude of change between the conditions for each feature. On the other hand, the *y*-axis indicates the level of significance, The dashed line is equivalent to a *p*-value of 0.05. Significance is derived from −10 log(*p*-value) calculations.

Among the proteins identified both by spectral count and area under the curve integration, a total of eight proteins were selected for validation through Western blot (Figure 3) and the corresponding squares were framed on the volcano plots (Figure 2). Blue squares denote proteins that did not meet the criteria outlined in the Materials section in PEAKS due to identification in fewer than five samples per group or possessing a quality score below 4. The PVDF blots depicting the results obtained through spectral counting and Western blot quantification (after normalization through total protein count) are illustrated in Figure 3a. This correlation for MDH between both quantification methods equals a Pearson's coefficient of 0.89,

https://doi.org/10.1021/acsomega.3c06647
ACS Omega XXXX, XXX, XXX−XXX

(a)

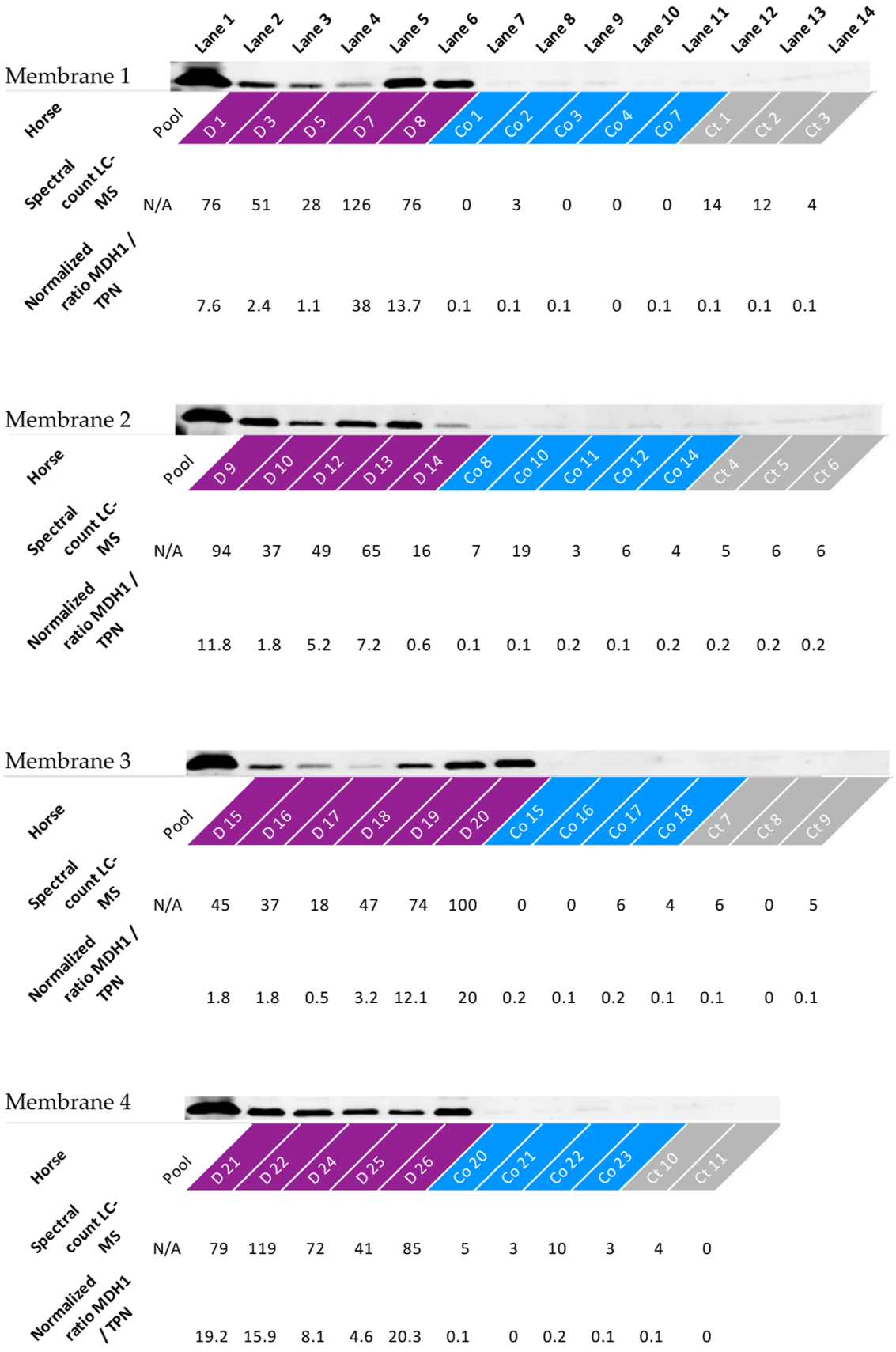

Figure 3. (a) Protein abundance of malate dehydrogenase 1 (MDH1, 36 kDa) was assessed across 50 serum samples using PVDF membranes in Western blot analysis. Prior to visualization as a scatter plot, Western blot analysis was normalized across membranes using the pool ratio (MDH1/total protein normalization). For each PVDF blot, the MDH1/TPN (total protein normalization) ratio is presented, along with the corresponding

https://doi.org/10.1021/acsomega.3c06647
ACS Omega XXXX, XXX, XXX−XXX

Figure 3. continued

spectral count quantified by LC−MS after identification using Mascot; (b) scatter plot illustrating the ratio between proteins of interest and the total protein count as determined by Western blot analysis. Each data point on the plot represents an individual horse, with diseased horses marked as "D," cograzing horses as "Co," and control horses as "Ct." Horizontal lines indicate the means for each respective group.

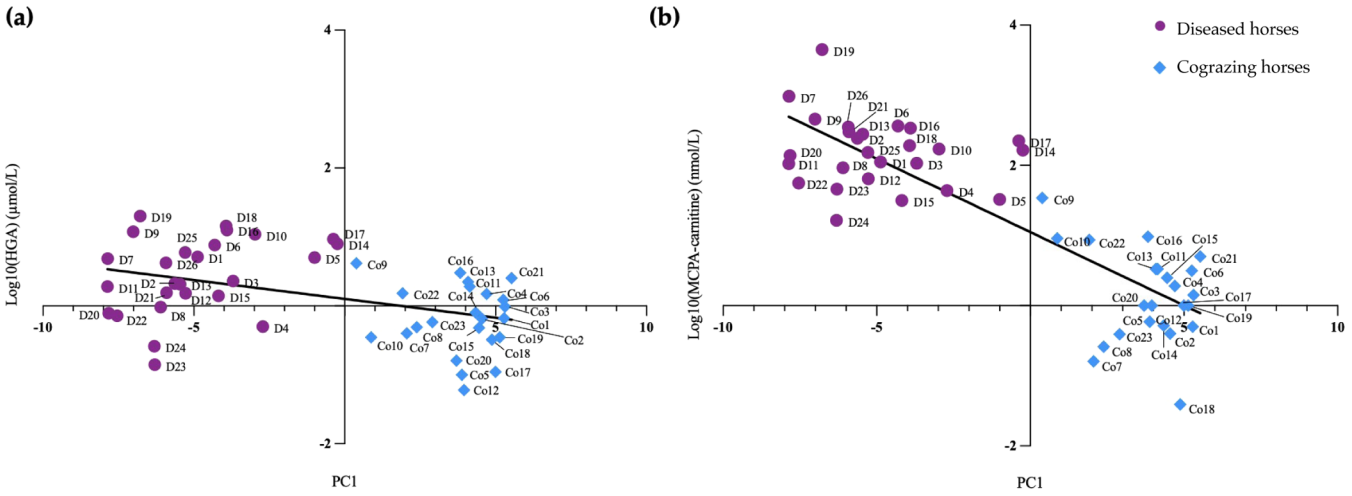

Figure 4. (a) Logarithmic HGA concentrations as a function of principal component 1 of PCA considering 245 proteins and (b) logarithmic MCPA-carnitine concentrations as a function of principal component 1 of PCA considering 245 proteins.

which indicates a strong correlation between variables.[39] The obtained ratios for each individual horse are listed in Figure 3b. Among the eight proteins tested, five demonstrated significant differences between diseased and clinically healthy horses (MDH1, APOA-IV, PRXD-6, LDH, and vitronectin). However, the quality of the von Willebrand factor seemed to be insufficient for further exploitation in this study.

To further elucidate the relevance of these proteins, a heatmap was generated in Figure 2c−e, based on their expression patterns. Proteins exhibiting similar expression trends across samples were clustered together by using hierarchical clustering. This clustering was performed using a neighbor-joining algorithm, employing a log 2 Euclidean distance similarity measure of the protein ratio for each group of horses compared to the average ratio. Furthermore, conditions from different samples were also clustered if they showed similar expressions across protein groups.[40]

In Figure 2c, the clustering of horses is predominantly based on their status, either AM or cograzers. However, there are minor instances of overlap, particularly at the point of passage, where horse 5, belonging to the diseased group, is clustered with the healthy cograzers. The same trend can be observed in Figure 2e, which includes all three analyzed groups. Except for horse 5, the horses belonging to the same categories are grouped together in Figure 2c. When all three categories are analyzed simultaneously (Figure 2e), AM horses are clustered together, while control and cograzing horses are combined. This representation highlights the separation of individual horses into clinically healthy (control and cograzing horses) and clinically diseased horses (AM horses).

3.2.2. Relationship between Proteomic Profile Analysis and Serum HGA/MCPA-Carnitine Levels. To analyze if the proteomes differ between groups, an unsupervised statistical method, i.e., a PCA, was used. This method allows a reduction of the dimensionality of large data sets to two principal components, allowing easier visualization of a multivariate data set with potentially intercorrelated variables.

The first PCA included only proteins that were identified in each individual horse (Figure 4a). On the *x*-axis, PC1 of the regression explains 55.05% of the differences between the individuals. It can be observed that PC1 is lower than 0 in all diseased animals, whereas it is above 0 in clinically healthy horses.

The second analysis considered all identified proteins regardless of whether they were identified in each group or in only one horse (Figure 4b). Even if the distinction between groups was not as clear as in the first PCA analysis, probably due to a lot of background proteins, it could be observed that diseased horses also distinguish from clinically healthy horses. Some diseased horses are at the threshold to clinically healthy ones, confirming the clustering of the heatmap and indicating that there seems to be a continuity of the proteome rather than clear-cut groups. Among the horses that are in-between of diseased and healthy horses are mainly surviving horses (horses 5, 14, and 17) and horse 4, which was euthanized against medical advice. Cograzers and control horses are mixed up, regardless of the type of PCA analysis, in line with the heatmap plotting of all 1965 identified proteins.

Since PC1 explains most of the variation in the data set (55.05%), a linear regression was performed plotting PC1 vs logarithmic values of HGA and MCPA-carnitine levels (Figure 4). Pearson's correlation coefficient (r, assuming normal distribution) was calculated for both analyses describing the strength and association between the variables. The coefficient between PC1 and $\log_{10}$ HGA was −0.43, indicating a moderate correlation between variables. Between PC1 and $\log_{10}$ MCPA-carnitine, the calculated correlation coefficient was −0.85, which is interpreted as a strong correlation.[39] Coefficients of determination (R^2) are 0.18 and 0.72, suggesting that about 72% of the variability of MCPA-carnitine concentrations in serum can be explained by PC1, rendering the exploration of proteins impacting PC1 indispensable (Table 2).

Among the proteins impacting most PC1 are eight proteins that belong to the glycolysis/gluconeogenesis pathway. Addi-

https://doi.org/10.1021/acsomega.3c06647
ACS Omega XXXX, XXX, XXX−XXX

Table 2. List of Proteins Identified through PCA of the 245 Proteins Present in Each Horse having a Pearson's Correlation Coefficient between −0.8 and −1(Figure 5a) , Indicating a Strong Negative Correlation

protein ID	Pearson coefficient to PC1	Pearson coefficient to PC2
cluster of glycogen phosphorylase[a]	−0.978096715	0.019569882
l-lactate dehydrogenase B	−0.972422423	−0.047994740
cluster of myosin-7 isoform X1	−0.969581298	−0.098449579
cluster of beta-enolase isoform X1[a,b]	−0.969323771	−0.033665667
fructose-bisphosphate aldolase A[a,b]	−0.966884020	−0.159152885
cluster of heat shock 70 kDa protein 1A	−0.958970179	0.001276235
phosphoglycerate mutase 2[a,b]	−0.953724799	0.079600972
malate dehydrogenase, cytoplasmic-like protein	−0.945990068	−0.027794134
cluster of aspartate aminotransferase, cytoplasmic[b]	−0.944715956	−0.017612607
cluster of tropomyosin beta chain isoform X4	−0.942698218	−0.119621223
cluster of CK M-type	−0.940136821	−0.084904065
cluster of myomesin-2 isoform X3	−0.940099429	−0.030437926
cluster of M1-type pyruvate kinase[b]	−0.937784199	0.148171735
cluster of glucose-6-phosphate isomerase[a]	−0.937031877	0.080341027
cluster of filamin-C isoform X3	−0.936441983	0.096328175
carbonic anhydrase 3	−0.935027301	0.125662913
14−3−3 protein epsilon isoform X2	−0.933444232	0.030888090
cluster of lactate dehydrogenase A	−0.931680766	0.221358313
cluster of phosphoglucomutase-1 isoform X2[a,b]	−0.922951966	0.171411080
cluster of titin isoform X50	−0.919073569	−0.104551540
heat shock 70 kDa protein 8	−0.918625505	0.039128239
cluster of heat shock protein HSP 90-alpha	−0.916285130	0.012113819
WD repeat-containing protein 1	−0.914785991	0.113181711
cluster of selenium-binding protein 1	−0.891307077	0.154948736
puromycin-sensitive aminopeptidase isoform X1	−0.848545367	−0.286241064
lipopolysaccharide-binding protein	−0.843994487	0.278775973
cluster of vinculin isoform X1	−0.839254527	0.112733266
cluster of plectin isoform X5	−0.811562489	−0.097632124
apolipoprotein A-IV	−0.809921946	−0.131493887

[a]Proteins that were identified as being significantly different between groups and belonging to the glycolysis/gluconeogenesis pathway. [b]Proteins involved in the biosynthesis of amino acids.

tionally, apolipoprotein A-IV is correlated with PC1 and overexpressed in AM horses, causing a possible increase in the secretion of triglycerides, cholesteryl ester, and phospholipids in the chylomicron particles.[41] This indicates an increase in triglycerides, which has been previously reported as a consequence of other toxicant-induced fatty acid β-oxidation inhibitions.[42]

3.2.3. Gene Ontology Analysis of Differentially Abundant Proteins. The biological relevance of the identified proteins was examined by using functional annotation through gene ontology. Gene ontology annotations allow for classification of proteins into three domains: biological processes, molecular function, and cellular components.

To visually depict the differential abundance of proteins between groups identified through spectral counting *t* tests, a hierarchical approach is employed. First, the presentation focuses on the repartition of biological processes. Second, the emphasis shifts to the primary modified biological pathways. Last, the distribution of pathway-relevant proteins in individual horses is illustrated.

For the comparison between AM and cograzers, the 230 DAPs were classified by the Panther protein class tool into 17 different protein classes of which 52 proteins were metabolite conversion enzymes, 30 were cytoskeletal proteins, and 26 were protein-modifying enzymes. Gene ontology biological pathway analysis identified that the main biological pathways involved either cellular or metabolic processes and biological regulation (102, 57, and 44 proteins, respectively) (Figure 5a). Cellular metabolic processes included cellular component organization (30 proteins), nitrogen compound metabolic processes (23 proteins), and heterocycle metabolic processes (19 proteins). Metabolic processes included organonitrogen compound metabolic processes (37 proteins), nucleobase-containing compound metabolic processes (17 proteins), and proteins involved in proteolysis (13 proteins). Regarding the proteins involved in biological regulation (34 proteins), most were involved in the regulation of cellular processes, such as proteolysis and cell surface-signaling pathways. Similar protein class repartition and gene ontology analysis were found when comparing AM horses to control horses (Figure 5b).

ShinyGO (0.76.1) was used for the graphical depiction of enrichment, matching gene characteristics, and protein interactions.[43] This tool facilitated the ability to analyze and comprehend biological pathways by locating differentially expressed proteins on KEGG pathways and mapping them based on the most enriched pathways.[36] The ShinyGO program examined "all available data sets" to assess the key differential paths across groups (i.e., KEGG, GO biological process, GO cellular component, and GO molecular function). The false discovery rate cutoff was set at 0.05, and the top 20 pathways are displayed. Multiple pathways are present in both group comparisons (AM vs cograzers and AM vs control horses) (Figure 6).

To confirm the biological significance of the proteomics data set, we extensively examined if previously reported findings in blood analyses of diseased horses[44−47] were also present in the proteomic analysis. Starting with CK (muscle type), we found a 22-fold elevation in AM horses compared to cograzers. Lactate dehydrogenase, a marker that is known to reach a peak 12 h after tissue injury, was also strongly elevated in diseased horses. Aspartate aminotransferase, the third enzyme analyzed in muscle pathologies, was less-frequently detected, presumably because of its later occurring peak, but was also significantly increased in AM horses ($p < 0.001$). As in common biochemistry blood tests, enzymes related to inflammation were increased in AM horses.

Serum amyloid A protein and fibrinogen, biomarkers of early signs of inflammation or sepsis, were significantly increased in diseased horses (normalized *t*-test, Benjamini−Hochberg correction $p < 0.01$).

3.2.3.1. Glycolysis/Gluconeogenesis. All DAPs were then used for the KEGG pathway analysis, and the relevant pathways were examined for biological interpretation.

In-depth investigation indicated a significant differential abundance of proteins involved in the glycolysis/gluconeogenesis (Figure 7), the coagulation and complement cascade (Figure 8), and biosynthesis of amino acids (Figure 9), which correspond to the three most modified pathways shown in Figure 6a. Spectral counting of concerned proteins is represented for each individual horse in Figures 7c, 8c, and 9c.

https://doi.org/10.1021/acsomega.3c06647
ACS Omega XXXX, XXX, XXX−XXX

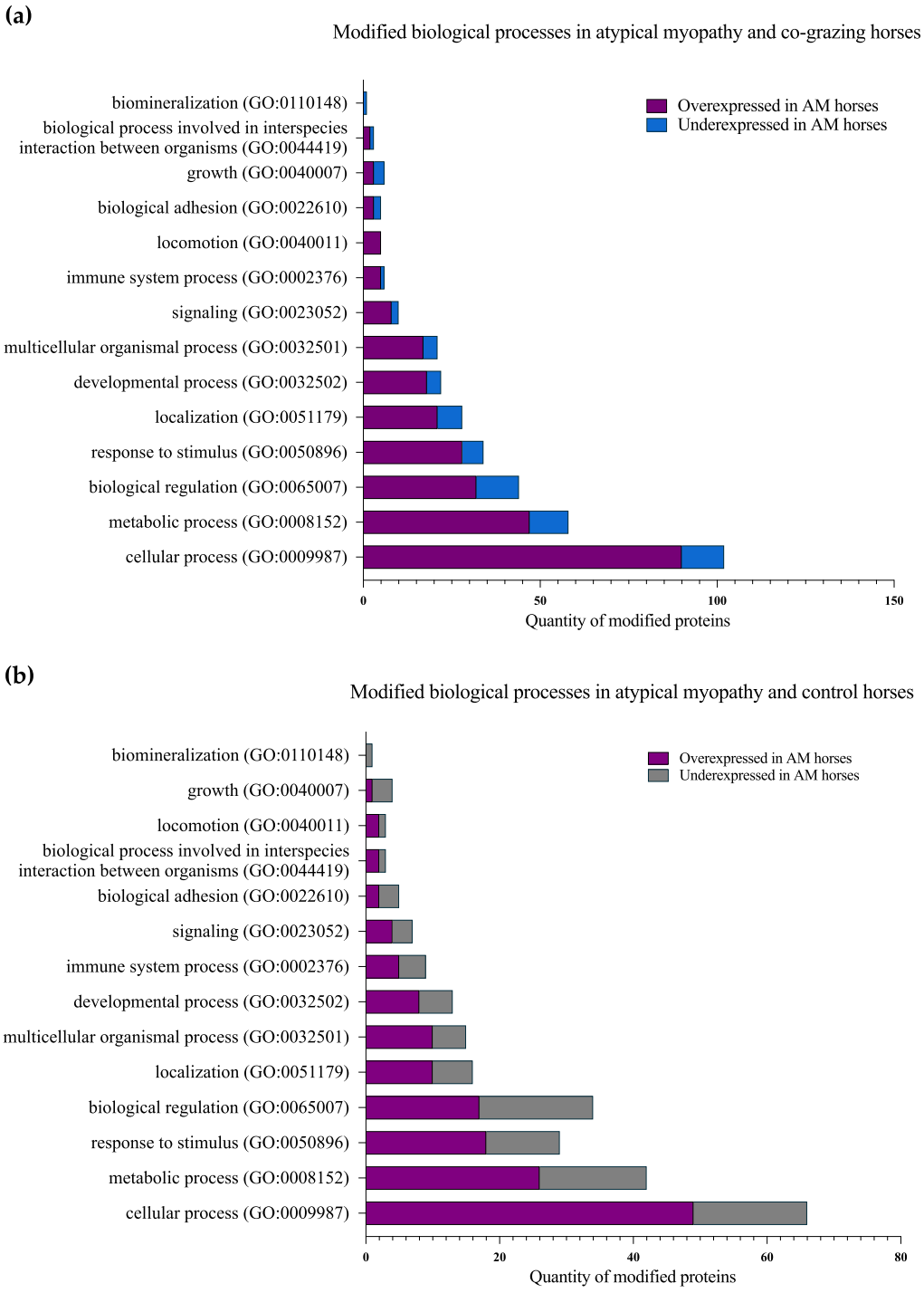

Figure 5. (a) Biological processes associated with the 230 DAPs between diseased animals (AM) and healthy cograzers and (b) biological processes associated with the 156 DAPs between diseased animals and control horses. AM: AM.

3.2.3.2. Complement Cascade/Coagulation. In the context of the coagulation and complement cascade, it was observed that all liver-synthesized proteins were diminished in the AM group. However, the von Willebrand factor, which is also produced by nonhepatic sinusoidal endothelial cells, showed an increase.[48] Coagulation abnormalities have been previously reported in cases of toxic or drug-induced hepatitis.[49] It is suggested that mild forms of hepatitis may exhibit a slight reduction in vitamin-K-related factors. However, as liver cell function further deteriorates, fibrinogen levels may rise, and von Willebrand factor becomes markedly elevated,[49] as observed in the group of AM horses.

Additionally, the AM horses demonstrated significantly higher levels of commonly used liver markers, such as aspartate aminotransferase and alanine aminotransferase. However, it is important to note that alanine aminotransferase was not detected in all diseased animals, which aligns with previous findings that increased liver enzyme activity is a frequent but not constant observation.[45]

3.2.3.3. Biosynthesis of Amino Acids. As HGA and MCPrG are converted through two enzymes also involved in the

https://doi.org/10.1021/acsomega.3c06647
ACS Omega XXXX, XXX, XXX−XXX

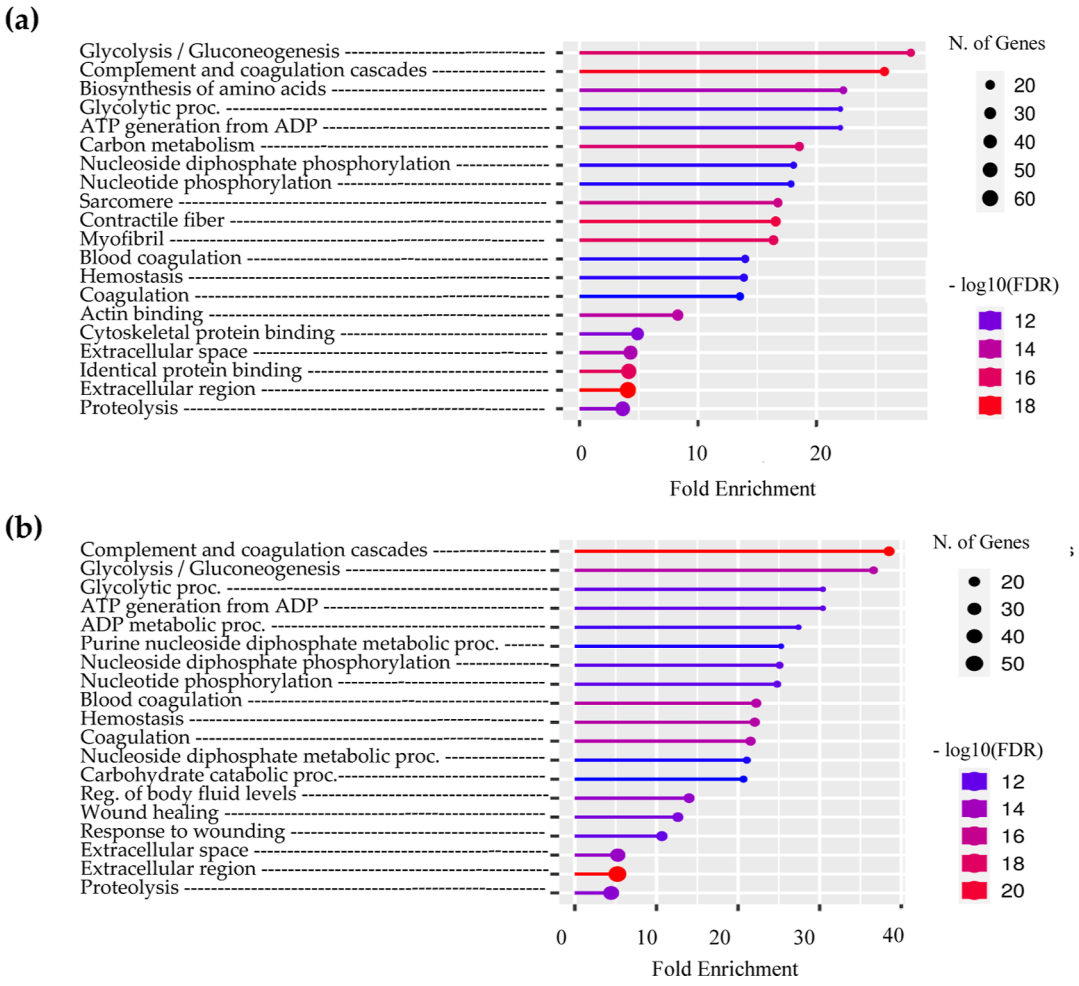

Figure 6. 20 most enriched pathways between (a) diseased horses and healthy cograzers and (b) diseased and control horses generated via ShinyGO (0.76.1).

metabolism of branched-chain amino acids,[6,8,9] this pathway warranted special attention. As previously stated, mitochondrial enzymes, specifically BCATm and BCKDHc, not only mediate the conversion of the protoxins into their toxic metabolites but also play a crucial role in the catabolism of essential proteinogenic amino acids, namely, leucine, isoleucine, and valine. These three BCAAs are vital components in protein synthesis pathways.[50,50]

In the context of the biosynthesis pathway of amino acids, a general increase in the expression of enzymes was observed, which supports previous findings in rats following MCPA poisoning.[6] However, interpreting this overall upregulation is challenging due to the identification of only cytosolic (iso-)enzymes. The limited detection of mitochondrial isoforms using this technique, which did not involve the depletion of highly abundant serum proteins, adds to the complexity. Considering that branched-chain amino acids are primarily catabolized by mitochondrial enzymes, their absence in serum detection does not necessarily imply their absence in the system. Instead, it suggests that these enzymes were not sequenced, potentially due to limitations in the dynamic range that hindered their adequate detection.

Regarding the proteins identified in the glycolysis pathway, there is considerable variation in the spectral counts of proteins associated with the biosynthesis of amino acid pathway among individuals. The individuals that exhibited only minor increases in glycolytic enzymes also displayed negligible levels of enzymes involved in amino acid biosynthesis.

3.2.3.4. Other Differentially Abundant Protein Groups. In agreement with the clinical manifestations of rhabdomyolysis in AM, several proteins related to the release of toxic intracellular material into the blood circulation were identified. The pathogenic base of rhabdomyolysis after toxic consumption is caused either by an impeded energy production or a direct lysis of the plasma membrane in skeletal muscle.[51] As the toxic metabolites incriminated in AM affect fatty acid β-oxidation, a reduced energy production can cause energy-dependent ion pump dysfunction, leading to an increase of intracellular Na^+ concentration, which in turn leads to a secondary cytosolic Ca^{2+} increase. When a critical limit of cytosolic Ca^{2+} is reached, a cascade of cellular death is activated[52,53] and as mitochondria are progressively damaged, the release of cytochrome *c* is induced, which acts as a pro-apoptotic factor.[51,53,54] Cytochrome *c* was found to be significantly increased in AM horses ($p < 0.001$). Another characteristic of mitochondrial calcium increase is the elevated production of reactive oxygen species (ROS),[55] which will be discussed further. Other proteins related to rhabdomyolysis were also identified, such as carbonic anhydrase III, which is found exclusively in skeletal muscle,[56] heavy-chain myosin fragments,[57] as well as lactate dehydrogenase and aspartate aminotransferase, as previously mentioned.

https://doi.org/10.1021/acsomega.3c06647
ACS Omega XXXX, XXX, XXX−XXX

(a)

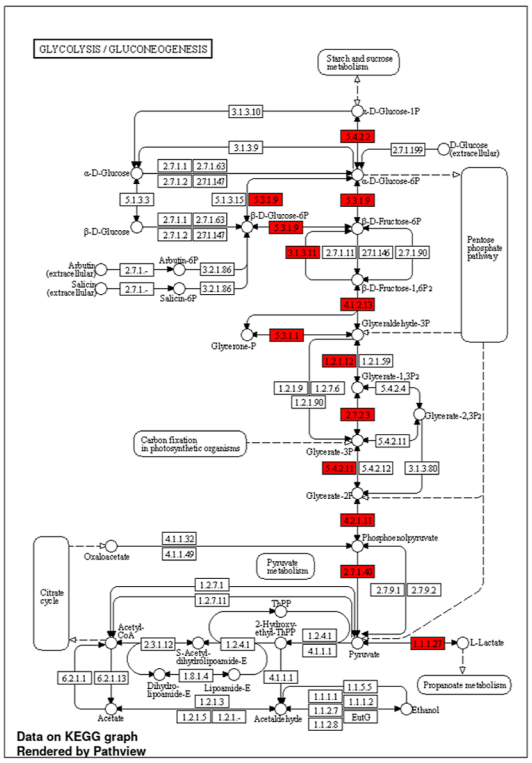

(b)

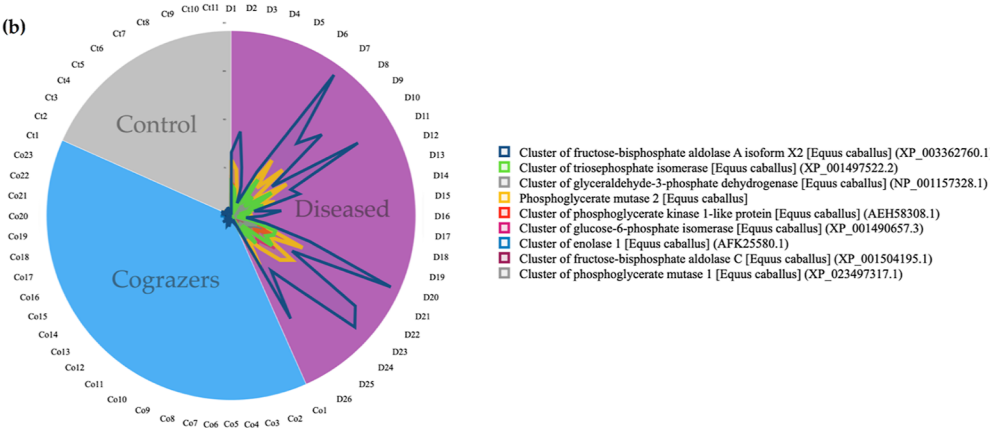

(c)

Protein / Enzyme	Panther protein class	Over/Under-expression in diseased horses
Fructose-bisphosphate aldolase A*	Aldolase	Overexpression
Fructose-bisphosphate aldolase B	Aldolase	Overexpression
Fructose-bisphosphate aldolase C*	Aldolase	Overexpression
Enolase 1*	Lyase	Overexpression
Enolase 3*	Lyase	Overexpression
Fructose biphosphatase 1	Carbohydrate phosphatase	Overexpression
Glucose 6-phosphate isomerase*	Isomerase	Overexpression
Glyceraldehyde-3-phosphate dehydrogenase*	Dehydrogenase	Overexpression
Lactate dehydrogenase A*	Dehydrogenase	Overexpression
Lactate dehydrogenase B*	Dehydrogenase	Overexpression
Phosphoglucomutase 1*	Mutase	Overexpression
Phosphoglycerate kinase*	Kinase	Overexpression
Phosphoglycerate mutase 1*	Mutase	Overexpression
Phosphoglycerate mutase 2*	Mutase	Overexpression
Pyruvate kinase*	Kinase	Overexpression
Triosephosphate isomerase 1*	Isomerase	Overexpression

Figure 7. (a) DAPs between AM diseased and cograzing horses in the glycolysis/gluconeogenesis pathway. DAPs between AM and control horses are marked with an asterisk (*). (b) KEGG glycolysis/gluconeogenesis pathway. Overexpressed proteins are presented in red. Reprinted with permission from Kanehisa, M.; Furumichi, M.; Sato, Y.; Kawashima, M.; Ishiguro-Watanabe, M.; KEGG for taxonomy-based analysis of pathways and genomes. Copyright 2023 Kanehisa Laboratories. (c) Radar diagram representing individual spectral counts for each protein of the above-mentioned pathway. AM-diseased horses are represented by numbers D1 through D26, healthy cograzers by numbers Co1 through Co23, and control horses by numbers Ct1 through Ct11.

https://doi.org/10.1021/acsomega.3c06647
ACS Omega XXXX, XXX, XXX−XXX

(a)

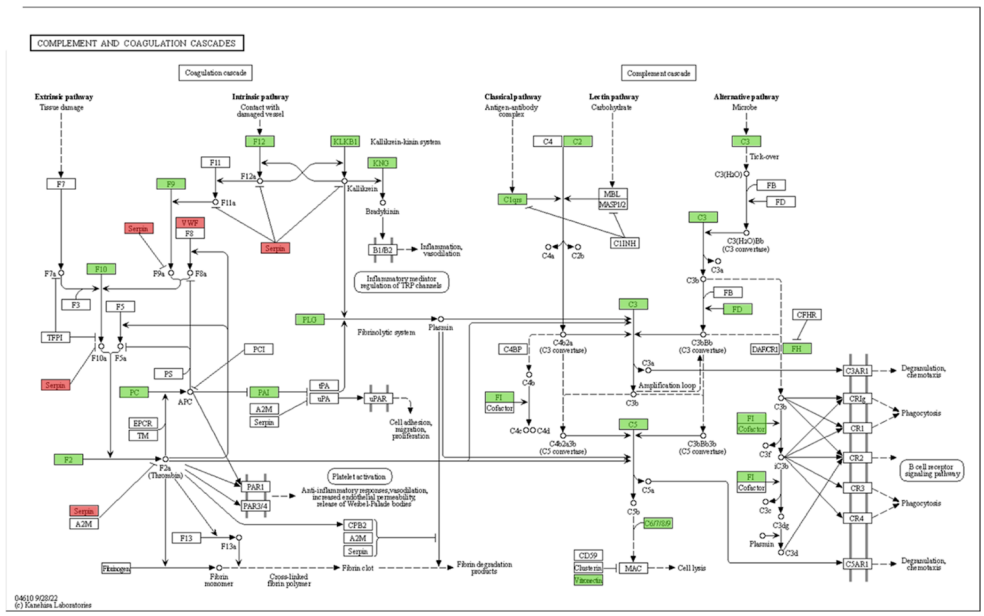

(b)

Protein / Enzyme	Panther protein class	Over/Under-expression in diseased horses
Thrombin (factor II)*	Serine protease	Underexpression
Coagulation factor IX*	Serine protease	Underexpression
Coagulation factor X*	Serine protease	Underexpression
Coagulation factor XII*	Serine protease	Underexpression
Complement C1r subcomponent*	Serine protease	Underexpression
Complement C2*	-	Underexpression
Complement C3-like*	Protease inhibitor	Underexpression
Complement C5	Protease inhibitor	Underexpression
Complement C8 alpha chain	Complement component	Underexpression
Complement factor D*	Serine protease	Underexpression
Complement factor I*	Serine protease	Underexpression
Complement factor H*	Complement component	Underexpression
Kallikrein B1*	Serine protease	Underexpression
Kininogen 1*	Protease inhibitor	Underexpression
Plasminogen*	Serine protease	Underexpression
Vitamin K-dependent protein C*	Serine protease	Underexpression
Antithrombin-III*	Protease inhibitor	Underexpression
Serpin family B member 10	Protease inhibitor	Overexpression
Leukocyte elastase inhibitor *	Protease inhibitor	Overexpression
Vitronectin*	-	Underexpression

(c)

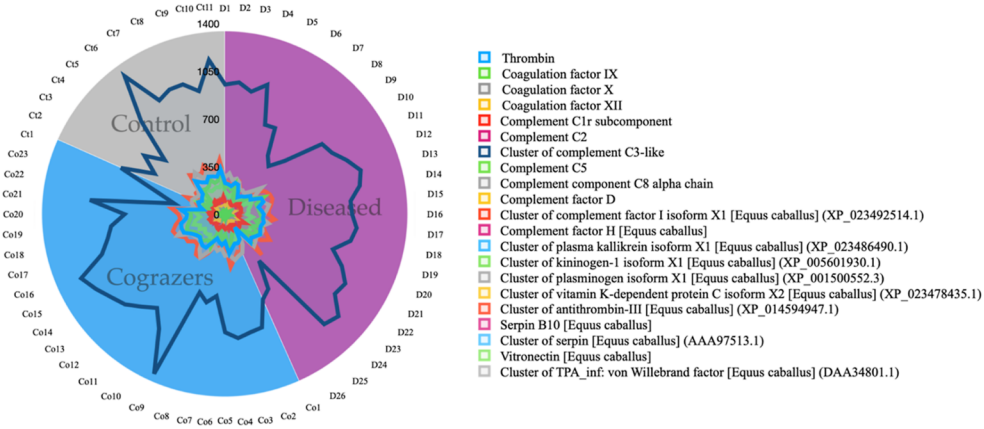

Figure 8. (a) DAPs between AM diseased and cograzing horses in the complement cascade/coagulation pathway. DAPs between AM and control horses are marked with an asterisk (*). (b) KEGG complement cascade/coagulation pathway. DAPs are presented in red. Reprinted with permission from Kanehisa, M., Furumichi, M., Sato, Y., Kawashima, M. and Ishiguro-Watanabe, M.; KEGG for taxonomy-based analysis of pathways and genomes. Copyright 2023 Kanehisa Laboratories. (c) Radar diagram representing individual spectral counts for each protein of the above-mentioned pathway. AM-diseased horses are represented by numbers D1 through D26, healthy cograzers by numbers Co1 through Co23, and control horses by numbers Ct1 through Ct11.

As presented in other types of equine myopathies, several inflammation proteins were increased in affected horses.[58,59] Interestingly, while in equine myofibrillar myopathy, muscle tissue is characterized by a decrease in the abundance of peroxiredoxin 6, a cytoprotective peroxidase, able to reduce hydrogen peroxides as well as phospholipid hydroperoxides,[59] in

https://doi.org/10.1021/acsomega.3c06647
ACS Omega XXXX, XXX, XXX−XXX

(a)

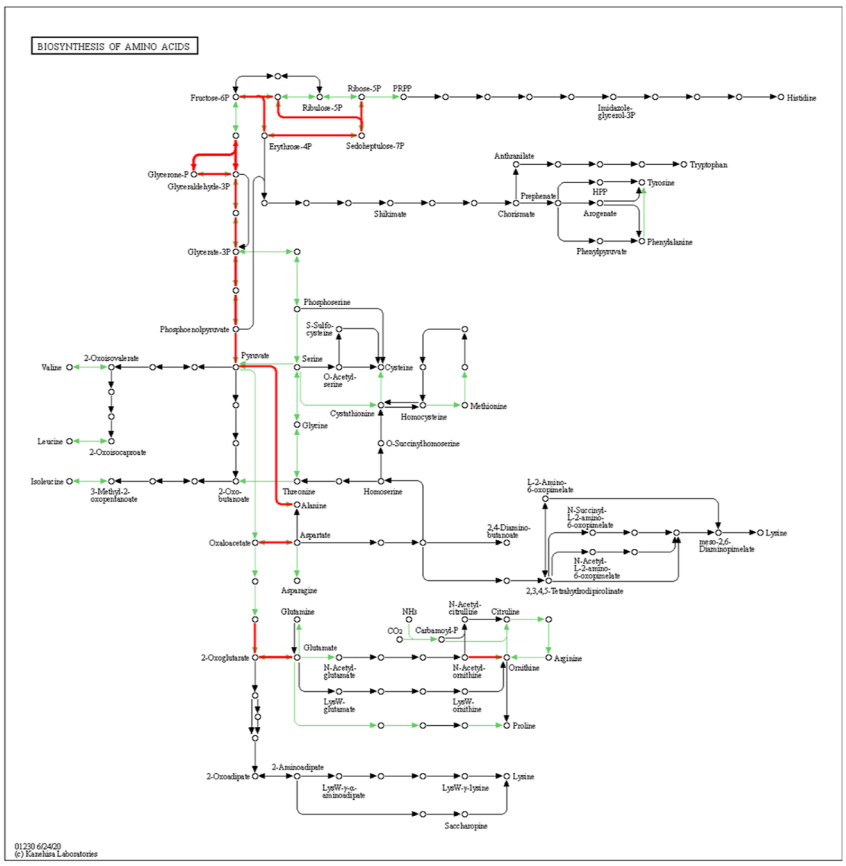

(b)

Protein / Enzyme	Panther protein class	Over/Under-expression in diseased horses
Fructose-bisphosphate aldolase A*	Aldolase	Overexpression
Fructose-bisphosphate aldolase B	Aldolase	Overexpression
Fructose-bisphosphate aldolase C*	Aldolase	Overexpression
Aminoacylase 1	Dehydrogenase	Overexpression
Enolase 1*	Lyase	Overexpression
Enolase 3*	Lyase	Overexpression
Glutamic-pyruvic transaminase (gpt/alt)	Isomerase	Overexpression
Glutamic-oxaloacetic transaminase 1 (got1/ast)*	Isomerase	Overexpression
Glyceraldehyde-3-phosphate dehydrogenase*	Dehydrogenase	Overexpression
Isocitrate dehydrogenase	Dehydrogenase	Overexpression
Phosphoglycerate kinase*	Kinase	Overexpression
Phosphoglycerate mutase 1*	Mutase	Overexpression
Phosphoglycerate mutase 2*	Mutase	Overexpression
Pyruvate kinase M1*	Kinase	Overexpression
Transaldolase	Aldolase	Overexpression
Transketolase	Transketolase	Overexpression
Triosephosphate isomerase 1*	Isomerase	Overexpression

(c)

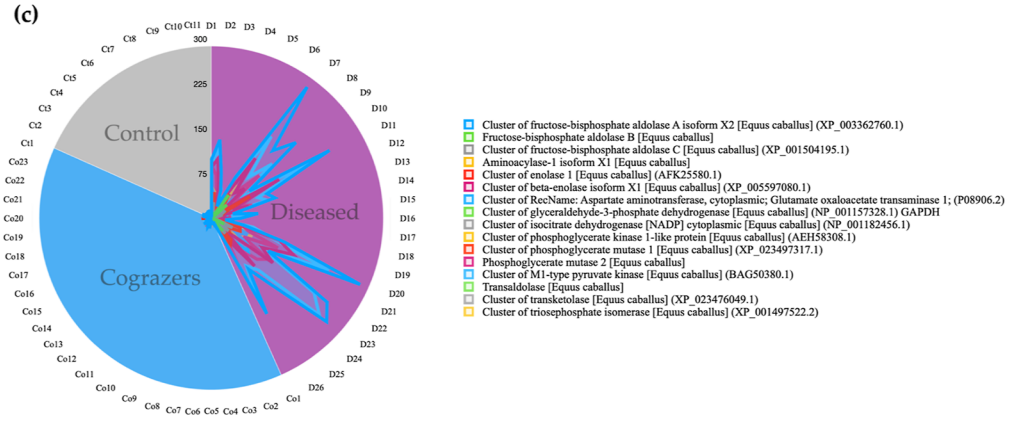

Figure 9. (a) DAPs between AM diseased and cograzing horses in the amino acid biosynthesis pathway. Upregulated pathways in diseased horses are marked in red. (b) KEGG amino acid biosynthesis pathway is illustrated in green. DAPs are presented in red. Reprinted with permission from Kanehisa, M., Furumichi, M., Sato, Y., Kawashima, M. and Ishiguro-Watanabe, M.; KEGG for taxonomy-based analysis of pathways and genomes.

https://doi.org/10.1021/acsomega.3c06647
ACS Omega XXXX, XXX, XXX−XXX

Figure 9. continued

 (c) Radar diagram representing individual spectral counts for each protein of the above-mentioned pathway. AM-diseased horses are represented by numbers D1 through D26, healthy cograzers by numbers Co1 through Co23, and control horses by numbers Ct1 through Ct11.

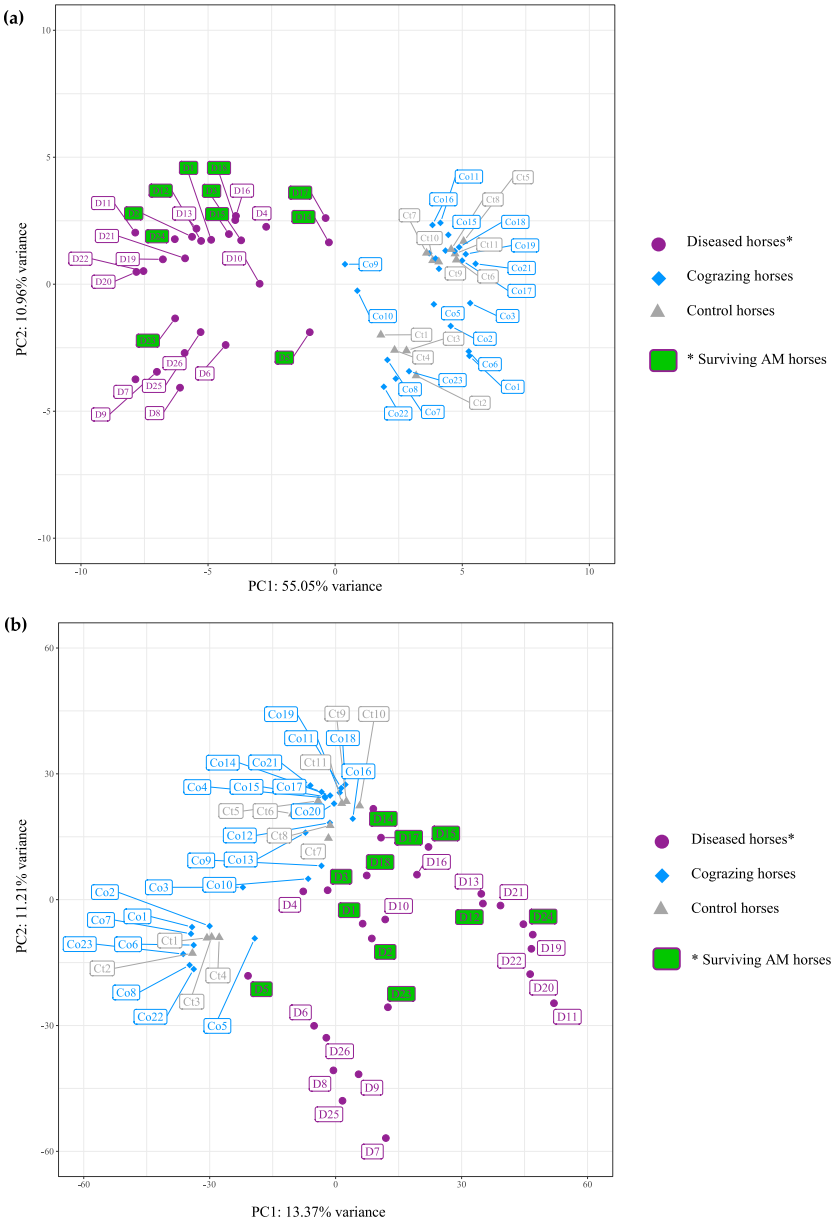

Figure 10. (a) PCA of the 245 proteins identified in each individual horse (no missing value) via Perseus and (b) PCA plot of all 1965 identified proteins via Perseus. Blue diamonds represent cograzing horses, gray triangles represent control horses, and purple circles represent diseased horses with survivors highlighted in green. Individuals with name annotation have been identified for comparison purposes between figures. Principal components 1 and 2 illustrate the proportion of variance explained by the eigenvector in the *x* and *y* axes.

this study, we show that horses affected with AM show an increase in serum peroxiredoxin 6.

Previous studies showed that the supplementation of vitamin complexes and antioxidant mixtures seemed to ameliorate the possible outcome of the disease.[21,60] This concurs with our findings as several key components of antioxidant defense mechanisms are activated in AM diseased horses. Similarly, lipid peroxidation is increased in plasma of horses affected by motor neuron disease, a neuromuscular disease, making oxidative stress a plausible contributor to disease development.[61] In the present study, a significant increase of both copper/zinc superoxide dismutase, a cytosolic enzyme that catalyzes the superoxide free radical ($O_2^{\bullet -}$) into H_2O_2 and O_2,[62] is observed in diseased horses. Also, an increase of glutathione transferases (GSTs), enzymes that catalyze glutathione conjugation, the first step of the mercapturic pathway, an essential detoxification process, is observable.[63] Among others, lipid peroxidation can be countered by GST activity.[64] In our study, three classes of GSTs were increased in diseased animals, namely, Mu, Pi, and Omega. In certain cancers, GST-Pi expression was upregulated

https://doi.org/10.1021/acsomega.3c06647
ACS Omega XXXX, XXX, XXX−XXX

in cancers exhibiting higher oxidative stress.[65] Regarding the cell signaling implications, in the case of an increase in ROS or specific drugs, the protein/protein interaction between GST-Pi and Jun-terminal kinases (JNK), involved in the MAPK pathway, dissociates. The resulting GST-Pi oligomers accumulate and JNK is activated, which can result in cell apoptosis.[66] Additionally, as in equine recurrent exertional rhabdomyolysis, thioredoxin, another marker of oxidative stress, was upregulated.[67]

Serum cystatin c can be used as a sensitive marker for renal damage and was significantly higher in diseased horses compared to healthy cograzers (*t*-test with Benjamini–Hochberg correction, $p < 0.01$). However, this marker is also correlated with an increase of C reactive protein (which was also observed in this data set) and must be therefore interpreted with caution. Novel biomarkers of kidney failure as symmetric dimethylarginine were not identified in any of the three groups. Neutrophil gelatinase-associated lipocalin, a protein produced by injured nephron epithelia, was significantly increased in AM horses ($p < 0.005$) compared to healthy cograzers. According to clinical studies, this protein is responsive to tissue stress and nephron injury and less to hemodynamic responses as creatine.[68] However, this potential biomarker is an acute phase reactant, which is also released by immune cells and liver in cases of sepsis.[68,69] Interestingly, this neutrophil gelatinase-associated lipocalin was also found to be increased in cograzing horse 9 (Co9), the horse that also had an overall proteomic profile which was closest to diseased AM horses (Figures 3 and 10).

3.2.4. Proteomic Pattern Analysis in "Cograzing Horses" vs "Control Horses". Spectral counts of all identified proteins were normalized for *t* testing and 42 proteins were identified as significantly different between groups ($p < 0.05$) (data set available via ProteomeXchange).

An increase in immunoglobulins and complement factors was observed, which may be due to complement activation after toxin ingestion.

Cystathionine beta-synthase, a pivotal enzyme of the transsulfuration pathway, was found to be decreased in AM horses compared to controls. This enzyme, which catalyzes the conversion of homocysteine to cystathionine, is also a precursor of glutathione, taurine, and H_2S. Even if increased taurine levels in AM horses[70] may originate from type-1 fiber rhabdomyolysis,[71] as glutathione was also increased in diseased horses, this overexpression may be an indicator of an early response to the ingested toxins.

4. DISCUSSION

The present study is the first comparing the serum proteome of horses suffering from AM, healthy cograzers, and control horses. Diseased horses had considerably higher protein expressions than the other groups with regard to cellular metabolic processes such as cell death, cytoskeletal structure, and energy-related metabolism.

Previous research by Westermann (2011) suggested that muscle glycogen concentrations would drop because glycogenolysis and glycolysis are triggered in response to reduced ATP concentrations.[11] Hyperglycemia is a common finding in AM.[45] Elevated blood glucose levels have also been found in several other studies of horses suffering from rhabdomyolysis with the tentative explanation that the gluconeogenic effect of plasma cortisol may be responsible for this increase.[72] Conversely, enzymes involved in glucose metabolism may leak out of muscle due to rhabdomyolysis, which could be at the origin of the observed increase in enzymes involved in glycolysis. This would also explain why glycogen depletion was observed in skeletal muscle fibers of diseased AM horses,[13] even though pathway-involved proteins were detected in the serum (Figure 6). Additionally, glucose entry into cells may be limited through the translocation of the glucose transporter 4, the main glucose carrier isoform in skeletal muscle, and therefore contributes to hyperglycemia.[73−75]

The higher abundance of proteins in diseased horses could therefore originate from rhabdomyolysis but also from different sources, such as an inflammatory reaction or the release of specific molecules due to muscle injury. The increased level of protein release linked to rhabdomyolysis involves the release of intracellular proteins into the bloodstream. These intracellular proteins, encompassing structural proteins, enzymes, and myoglobin, are typically absent or present at very low, often undetectable levels in healthy individuals. The release of a large number of intracellular proteins increases the pool of proteins available for identification in serum proteomic analysis.

As rhabdomyolysis triggers an inflammatory response, inflammation can lead to the activation and recruitment of immune cells, leading to the release of cytokines, chemokines, and other signaling molecules into the bloodstream. Consequently, immune- and inflammation-related proteins such as neutrophil gelatinase-associated lipocalin, metalloproteinases, and diverse interleukines were detected and identified in the serum proteomic analysis, contributing to an increased number of identified proteins. This finding was further supported by gene ontology analysis, revealing upregulated pathways related to inflammation processes.

A notable advantage of proteomics lies in its ability to discern distinct isoforms. When multiple isoforms are detected for specific proteins, their origins can be traced. In our study, we detected an increased abundance in CK-M (skeletal muscle and myocardium) but also, in some AM horses, of the CK-B (brain and smooth muscle) type. Therefore, it seems that diseased horses show an increase in CK not only due to rhabdomyolysis but also due to smooth muscle injury or cellular leakage caused by the disruption of cell membranes. Additionally, the cellular location can dictate a protein's role. As such, cytosolic MDH1 plays a significant role in the malate/aspartate shuffle. Yet, this protein may either leak from injured tissues, reflecting cellular damage and subsequent release of cellular contents, including MDH1, into the bloodstream, or originate from organ dysfunction. While an overall increase in MDH1 was observed in diseased horses, individual spectral count analysis also revealed substantial elevation in Co9 and Co10, which exhibited proteomes closely resembling those of the diseased horses. Furthermore, the study identified certain enzymes such as vitronectin with decreased levels in affected horses, pointing toward a potential decline in production. This indicates that these phenotypically healthy horses had already experienced tissue-related changes, indicating that there does not seem to be a specific "onset" of the disease. While we recognize that we possess only partial information on the overall progression of the disease, our results do imply metabolic consequences in cograzers following toxin ingestion. However, it is essential to clarify that our data do not enable us to definitively assert a gradual progression of the disease as this would require a more extensive temporal analysis and the outcome following toxin ingestion of individual horses being multifaceted.

https://doi.org/10.1021/acsomega.3c06647
ACS Omega XXXX, XXX, XXX−XXX

When information about isoforms and cellular origin is not available, the exact source cannot be conclusively ascertained. So, while the overall surge of enzymes belonging to the glycolysis/gluconeogenesis pathway could indicate an energy switch that would most likely be brought on by the well-known inhibition of fatty-acid β-oxidation, multifunctional proteins may possibly harbor additional functions. For instance, the activities of alpha-enolase (ENO1) greatly fluctuate depending on its localization. Even though the primary function is catalysis of glycolysis, ENO1 can also act as a plasminogen receptor, promote extracellular matrix degradation, maintain mitochondrial membrane stability, regulate signaling pathways as PI3K-AKT/AMPK-mTOR, or simply organize microtubules.[76] These potential additional effects must therefore be considered in the interpretation of the molecular consequences of the toxins involved in AM.

Regardless, some enzymes known to be synthesized in the liver as several coagulation factors were markedly decreased in diseased horses. Interestingly, among the first reported Belgian AM cases 20 years ago, some diseased horses showed petechia at autopsy, i.e., signs of disseminated intravascular coagulation (DIC).[13] This DIC is also a complication in human myopathies and is thought to originate from an activation of the coagulation cascade by components released from the damaged muscles.[77] Even if DIC can resolve spontaneously in human cases of rhabdomyolysis, platelet therapy, fresh frozen plasma, and vitamin K administration have been described in cases where hemorrhagic complications occurred, particularly when the underlying cause could not be corrected.[77] It remains unclear whether these findings are coincidental or related to a more acute and therefore rapid course of the disease 20 years ago as this finding in autopsy has become uncommon (unpublished data). Another hypothesis is that both coagulation factors and enzymes involved in the complement system are less present in AM horses' serum because the factors are depleted. Because we analyzed sera collected at a specific time point, no deduction of the specific kinetics of enzymes can be made. A decrease in hepatic coagulation factors, associated with significantly elevated liver enzymes in the present study, would however indicate that the toxins are not only metabolized within the liver but also cause signs of an induced acute hepatic dysfunction. In humans, hepatic dysfunction has been described as a complication in approximatively 25% of rhabdomyolyses with the hypothesis that proteases released from injured muscles might cause this transient dysfunction.[78]

Impaired fatty acid β-oxidation can lead to the accumulation of free fatty acids in the cytoplasm, and their subsequent esterification as triglycerides to prevent FFA-associated cytotoxicity contributes to drug-induced steatosis.[79] Previous studies have reported histological findings on the hepatic level (i.e., acute portal congestion and lipidosis), but these findings were not observed in every individual.[13,60] As hepatotoxic damage in the form of steatosis is usually observed after repeated or long-term exposition (i.e., several weeks, even months) to a drug[79,80] and that AM horses are grazed all year round, the duration of exposition is probably not the adequate explanation. The proteome as well as histopathological features vary between individuals, and the clinical profile of AM horses seems to be inconsistent and has evolved over the past 20 years.

In light of the hypothesis that incriminated toxins are metabolized by mitochondrial enzymes (i.e., BCATm and BCKDHc, respectively), the question of the impact on the mitochondria was raised. However, this aspect cannot be analyzed in the present study because only a limited number of mitochondrial enzymes were identified. This is probably due to the dynamic range hindering adequate detection in serum.

However, the reaction module of 2-oxocarboxylic acid chain extension by the tricarboxylic acid pathway was upregulated in AM-affected animals. When chemistry-oriented modules in metabolic pathways are analyzed, some tandem reactions share the same order of organic chemistry reaction types. Therefore, pathways of 2-oxocarboxylic acid chain extension by tricarboxylic acid appear in the Krebs cycle, lysine biosynthesis, and branched-chain amino acid biosynthesis among others. By consumption of one acetyl-CoA, these routes extend various 2-oxocarboxylic acids. Even though they target distinct substrates and that their corresponding genes are not always allocated to the same ortholog groups, the organic chemistry processes of each reaction are the same,[81] making it possible to think that the mitochondrial enzymatic complex involved in the transformation of the toxins is also upregulated.

The surge of antioxidant enzymes within the proteomic profiles of the affected horses suggests an adaptive response to mitigate oxidative stress. This response aligns with analogous disturbances in pathways implicated in cellular and oxidative stress, as recently reported in cases of recurrent exertional rhabdomyolysis in horses.[82] However, the sufficiency of endogenous antioxidant upregulation for complete quenching of ROS remains unanswered. As supplementation of vitamin complexes and antioxidants has been reported to help increase antioxidant defenses in horses,[83] our findings lend further credence to previous research highlighting the positive impact of this type of supplements to AM-affected horses.[21,60]

Through PLS analysis, we were able to differentiate healthy from diseased horses (Figure 10). This unsupervised statistical method allowed to visualize the differences between the proteome of diseased horses but also showed a merge in the representation of cograzers and control horses. Furthermore, most of the diseased horses that survived were grouped closely to healthy horses. When analyzing individual variations between diseased horses, two horses stuck out. Horse 5 (D5) distinguishes itself from the other horses in the AM group. This horse was clustered with the group of healthy cograzing horses (Figure 2) and does not follow the same protein overexpression as other AM horses. In fact, horse 5 was a pregnant mare, showing compatible signs of sycamore-related poisoning. Indeed, all inclusion criteria were respected, which renders AM a highly probable diagnosis. However, through its distinction with other horses, another hypothesis is that this horse was suffering from nutritional myopathy. This particular type of rhabdomyolysis originates from a severe selenium deficiency, and although rare in adult horses, had been reported in a pregnant mare, also in association with a multiple acyl-CoA deficiency.[84]

Diseased horse 4 (D4), which was euthanized against medical advice, was grouped with surviving horses (Figure 10) and showed below group average increase of glycolytic enzymes (Figures 6 and 8), raising the question as to if this horse would not have survived the course of the disease.

Regarding healthy cograzing horses, horse 9 (Co9) was grouped closest to diseased AM horses (Figures 3 and 10). As this was also the only healthy horse with increased levels of neutrophil gelatinase-associated lipocalin, it is a potential early marker of kidney injury.

https://doi.org/10.1021/acsomega.3c06647
ACS Omega XXXX, XXX, XXX−XXX

5. CONCLUSIONS

The information regarding the exact localization of the proteins cannot be obtained through label-free proteomics, and therefore, the interpretation of possible roles is hypothetical. Additionally, it must be enhanced that the proteomic analysis performed on circulating serum proteins only represents a snapshot of in vivo flux. Indeed, analyses of blood constituents reflect what happens at an intersection, i.e., where organs release or take up biomolecules. The effects of the toxins on muscle or liver cells may therefore be very different.[85] Thus, the significance of blood constituents must be interpreted with caution.

However, it is of note that there is an increase in either protein production or at least protein release into the blood in AM horses (Appendix). Whether this increase is related to an activation of cell signaling pathways such as mTOR or simply to a generalized inflammation cannot be determined at this point.

Despite identifying proteins that differ significantly between cograzers and control horses, an unsupervised statistical approach such as PCA was unable to distinguish the two healthy groups based on the entire proteome. This leads to the conclusion that while certain proteins differ across groups, these differences are largely diluted when studying the entire proteome. Our data suggest repercussions on the metabolism in cograzers following toxin ingestion while not allowing us to confidently assert a gradual progression of the disease. To establish such a progression, a more comprehensive temporal analysis, specifically through a kinetic approach, would be required.

Additionally, certain glycolytic proteins can play the role of potential biomarkers regarding the course of the disease. A rapid detection of these enzymes not only indicates an energy switch but could also be indicators of a horse's prognosis criteria as these enzymes were more increased in horses that died. Furthermore, we were able to discriminate the difference in protein abundance between horse 5 (D5) and other diseased horses, emphasizing the usefulness of the analysis of the different metabolic pathways including, among others, glycolysis/gluconeogenesis.

In conclusion, inflammation and cell death are very probably a consequence of the acute intoxication and resulting rhabdomyolysis as similar findings were described in horses with exertional rhabdomyolysis.[67] Cell contact with cytotoxic agents result in a combination of inflammation, oxidative stress, and a high energy demand, which is probably trying to be met by enhanced glycolysis.

Through our results, the use of antioxidants can be justified and explains their previously reported favorable prognostic

Appendix

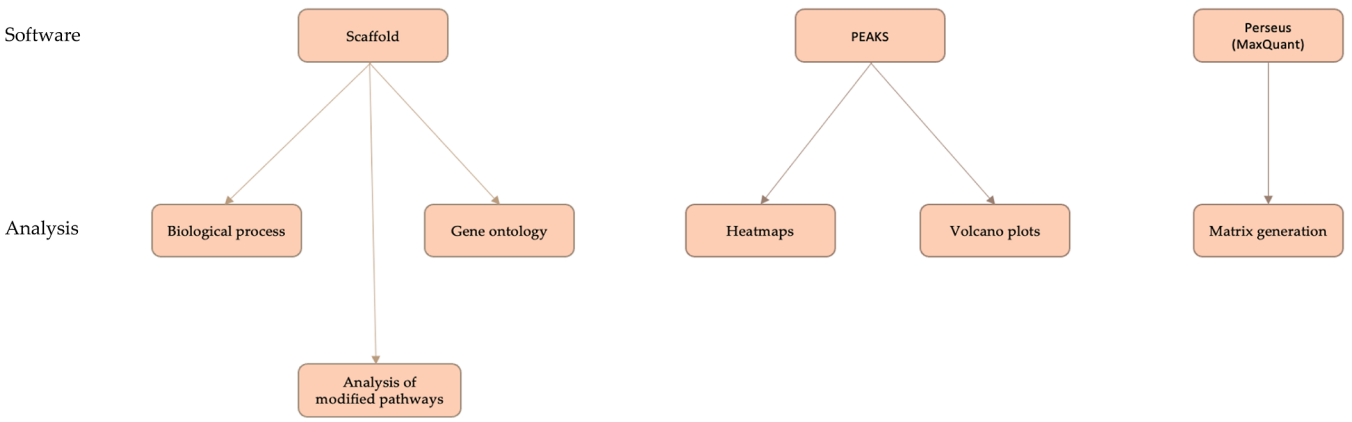

Figure 11. Summary of software and methods of analysis used in the present study.

Target	Manufacturer	Reference	Dilution factor
Malate dehydrogenase 1	Proteintech (Manchester, UK)	15904-1-AP	1:1000
Cystathionine ß-synthase	Proteintech (Manchester, UK)	14787-1-AP	1:1000
Apolipoprotein A-IV	Proteintech (Manchester, UK)	17996-1-AP	1:1000
Lactate dehydrogenase	Abcam (Cambridge, UK)	ab52488	1:500
Peroxiredoxin-6	Proteintech (Manchester, UK)	13585-1-AP	1:1000
Isocitrate dehydrogenase	Cell Signaling Technology (Danvers, MA, USA)	564395	1:1000
Von Willebrand factor	Abcam (Cambridge, UK)	ab6994	1:500
Vitronectin	Proteintech (Manchester, UK)	15833-1-AP	1:1000

Figure 12. Antibodies used for validation through Western blotting.

https://doi.org/10.1021/acsomega.3c06647
ACS Omega XXXX, XXX, XXX−XXX

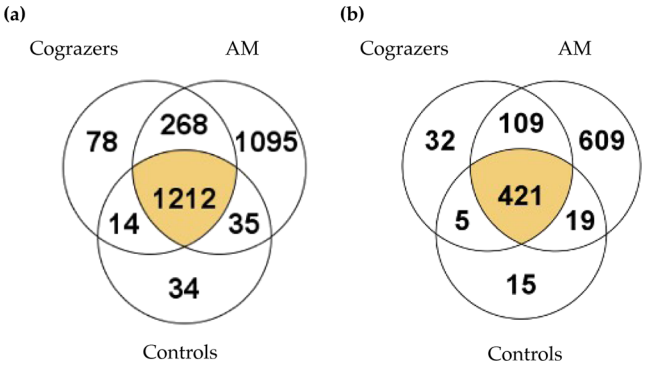

Figure 13. Venn diagram representing 2736 individual proteins (a) and 1210 protein family cluster (b) distribution between groups.

factor. Electrolyte imbalances should be closely monitored and, combined with adequate fluid therapy and vitamin complexes, might redirect the approach to slow down the organs' reaction to the deleterious effects of the incriminated toxins.

APPENDIX

Figures 11−13 and Table 3 are provided with additional data.

ASSOCIATED CONTENT

Data Availability Statement

All data supporting reported results can be found, including links to publicly archived data sets analyzed or generated during the study: data are available via ProteomeXchange with identifier PXD040429. Reviewer account details: .Username: reviewer_pxd040429@ebi.ac.uk. Password: VQ75rtY6.

Table 3. Demographic and HGA/MCPA-Carnitine Blood Level Data of Sampled Horses[a]

	SEX	AGE	HGA (μmol/L)	MCPA-carnitine (nmol/L)
CONTROL HORSES				
Ct 1	Mare	17		
Ct 2	Gelding	23		
Ct 3	Gelding	21		
Ct 4	Mare	12		
Ct 5	Mare	4		
Ct 6	Stallion	3	N/A	N/A
Ct 7	Gelding	4		
Ct 8	Stallion	12		
Ct 9	Stallion	3		
Ct 10	Mare	8		
Ct 11	Gelding	19		
MEAN ± SD		**11.5 ± 7.6**		
COGRAZING HORSES				
Co 1	Gelding	14	0.66	0.50
Co 2	Gelding	13	0.65	0.40
Co 3	Gelding	16	0.97	1.42
Co 4	Mare	20	1.49	1.90
Co 5	Stallion	1.5	0.10	0.59
Co 6	Mare	18	1.22	3.15
Co 7	Mare	29	0.40	0.16
Co 8	Mare	2	0.49	0.26
Co 9	Stallion	1	4.14	34.40
Co 10	Gelding	U	0.35	9.08
Co 11	Mare	5	1.91	7.91
Co 12	Gelding	17	0.06	0.00
Co 13	Gelding	U	2.23	3.34
Co 14	Mare	17	0.80	0.52
Co 15	Mare	17	0.48	2.49
Co 16	Gelding	20	3.01	9.59
Co 17	Gelding	20	0.11	0.00
Co 18	Gelding	18	0.32	0.04
Co 19	Gelding	21	0.35	0.00
Co 20	Gelding	16	0.16	0.00
Co 21	Gelding	20	2.53	5.02
Co 23	Mare	15	0.58	0.39
MEAN ± SD		**14.5 ± 7.5**	**1.1 ± 1.1**	**3.7 ± 7.5**
DISEASED HORSES				
D 1	Gelding	8.5	5.11	112.00
D 2	Mare	4	2.11	244.00
D 3	Gelding	6	2.29	107.00
D 4*	Gelding	13.5	0.50	43.70
D 5	Mare	21	5.03	32.70
D 6*	Gelding	5.5	7.62	363.00
D 7*	Mare	2	4.83	966.00
D 8*	Mare	13	0.96	92.50
D 9*	Stallion	7	11.90	457.00
D 10*	Stallion	1.5	10.90	171.00
D 11*	Stallion	1.5	1.90	106.00
D 12	Gelding	14.5	1.52	64.40
D 13*	Gelding	2	2.06	278.00
D 14	Stallion	2	7.97	165.00
D 15	Mare	8.5	1.40	31.50
D 16*	Gelding	7	12.60	339.00
D 17	Mare	12.5	9.26	224.00
D 18	Gelding	5	14.40	191.00
D 19*	Stallion	10	20.00	4480.00
D 20*	Mare	1	0.78	138.00
D 21*	Gelding	1.5	1.55	301.00
D 22*	Stallion	1.5	0.72	56.10
D 23	Mare	7	0.14	45.80
D 24	Gelding	1	0.26	16.50
D 25*	Stallion	3	5.94	153.00
D 26*	Gelding	4.5	4.22	352.00
MEAN ± SD		**6.3 ± 5.2**	**5.2 ± 5.2**	**366.5 ± 861.6**

[a]Age is given in years, HGA is given in μmol/L, and MCPA-carnitine in nmol/L. The last row of each group corresponds to column means ± standard deviation. Diseased horses marked with an asterisk died of AM or were euthanized during their hospitalization. Horse n°4 was euthanized against medical advice. N/A: not applicable; U: unknown.

https://doi.org/10.1021/acsomega.3c06647
ACS Omega XXXX, XXX, XXX−XXX

AUTHOR INFORMATION

Corresponding Author

Caroline-J. Kruse − *Department of Functional Sciences, Faculty of Veterinary Medicine, Physiology and Sport Medicine, Fundamental and Applied Research for Animals & Health (FARAH), University of Liège, 4000 Liège 1, Belgium;* orcid.org/0000-0003-4259-0988; Phone: +32 366 40 31; Email: caroline.kruse@uliege.be

Authors

Marc Dieu − *Namur Research Institute for Life Sciences (Narilis), University of Namur (UNamur), Namur 5000, Belgium; MaSUN, Mass Spectrometry Facility, University of Namur (UNamur), Namur 5000, Belgium*

Benoît Renaud − *Department of Functional Sciences, Faculty of Veterinary Medicine, Pharmacology and Toxicology, Fundamental and Applied Research for Animals & Health (FARAH), University of Liège, 4000 Liège 1, Belgium*

Anne-Christine François − *Department of Functional Sciences, Faculty of Veterinary Medicine, Pharmacology and Toxicology, Fundamental and Applied Research for Animals & Health (FARAH), University of Liège, 4000 Liège 1, Belgium*

David Stern − *GIGA Bioinformatics Platform, GIGA Institute, University of Liège, 4000 Liège, Belgium*

Catherine Demazy − *Namur Research Institute for Life Sciences (Narilis), University of Namur (UNamur), Namur 5000, Belgium; MaSUN, Mass Spectrometry Facility, University of Namur (UNamur), Namur 5000, Belgium*

Sophie Burteau − *Namur Research Institute for Life Sciences (Narilis), University of Namur (UNamur), Namur 5000, Belgium; MaSUN, Mass Spectrometry Facility, University of Namur (UNamur), Namur 5000, Belgium*

François Boemer − *Biochemical Genetics Lab, Department of Human Genetics, CHU of Liège, University of Liège, 4000 Liège, Belgium*

Tatiana Art − *Department of Functional Sciences, Faculty of Veterinary Medicine, Physiology and Sport Medicine, Fundamental and Applied Research for Animals & Health (FARAH), University of Liège, 4000 Liège 1, Belgium*

Patricia Renard − *Namur Research Institute for Life Sciences (Narilis), University of Namur (UNamur), Namur 5000, Belgium; MaSUN, Mass Spectrometry Facility, University of Namur (UNamur), Namur 5000, Belgium*

Dominique-M. Votion − *Department of Functional Sciences, Faculty of Veterinary Medicine, Pharmacology and Toxicology, Fundamental and Applied Research for Animals & Health (FARAH), University of Liège, 4000 Liège 1, Belgium*

Complete contact information is available at: https://pubs.acs.org/10.1021/acsomega.3c06647

Author Contributions

Conceptualization, C.K., M.D., P.R., and D.V.; methodology, C.D., S.B., M.D., and F.B; software, C.K. and M.D.; validation, C.K., M.D., C.D, and S.B.; formal analysis, C.K., M.D., D.S., and F.B.; investigation, C.K., C.D., M.D., and D.S.; resources, B.R. and A.-C.F.; data curation, C.K., M.D., and D.S.; writing—original draft preparation, C.K., D.V., M.D., C.D., and P.R.; writing—review and editing, C.K., M.D., B.R., A.-C.F, D.S., C.D., S.B., F.B., T.A., P.R., and D.V.; visualization, C.K., B.R., and P.R.; supervision, D.V. and T.A.; project administration, M.D., P.R., and D.V.; funding acquisition, D.V, T.A., and C.K. All authors have read and agreed to the published version of the manuscript.

Funding

The study was supported by the "la Wallonie agriculture SPW" (Service public de Wallonie; Belgique) and by "Les Fonds Spéciaux pour la Recherche (FSR)" of Liege University (Belgium). The first author (C.K.) is the recipient of a F.R.S-FNRS (Fonds de la recherche scientifique) research fellow grant.

Notes

The authors declare no competing financial interest.
Ethical review and approval were waived for this study since the blood sampling procedure is a part of routine veterinary practice to establish a diagnosis or to prevent AM.

ACKNOWLEDGMENTS

The authors would like to acknowledge Dr. Lola Dechêne for her incentives and thank Adeline Deward (Illumine) for the design of the graphical abstract.

REFERENCES

(1) Votion, D.-M.; van Galen, G.; Sweetman, L.; Boemer, F.; de Tullio, P.; Dopagne, C.; Lefèvre, L.; Mouithys-Mickalad, A.; Patarin, F.; Rouxhet, S.; van Loon, G.; Serteyn, D.; Sponseller, B. T.; Valberg, S. J. Identification of Methylenecyclopropyl Acetic Acid in Serum of European Horses with Atypical Myopathy. *Equine Vet. J.* **2014**, *46* (2), 146−149.

(2) Sander, J.; Terhardt, M.; Sander, S.; Aboling, S.; Janzen, N. A New Method for Quantifying Causative and Diagnostic Markers of Methylenecyclopropylglycine Poisoning. *Toxicol. Rep.* **2019**, *6*, 803−808.

(3) El-Khatib, A. H.; Engel, A. M.; Weigel, S. Co-Occurrence of Hypoglycin A and Hypoglycin B in Sycamore and Box Elder Maple Proved by LC-MS/MS and LC-HR-MS. *Toxins* **2022**, *14* (9), 608.

(4) Von Holt, C.; Holt, C. Methylenecyclopropaneacetic Acid, a Metabolite of Hypoglycin. *Biochim. Biophys. Acta* **1966**, *125*, 1−10.

(5) Melde, K.; Buettner, H.; Boschert, W.; Wolf, H. P. O.; Ghisla, S. Mechanism of Hypoglycaemic Action of Methylenecyclopropylglycine. *Biochem. J.* **1989**, *259* (3), 921−924.

(6) Melde, K.; Jackson, S.; Bartlett, K.; Sherratt, H. S. A.; Ghisla, S.; Ghisla, S. Metabolic consequences of methylenecyclopropylglycine poisoning in rats. *Biochem. J.* **1991**, *274*, 395−400.

(7) Sherratt, H. S. A. Hypoglycin, the Famous Toxin of the Unripe Jamaican Ackee Fruit. *Trends Pharmacol. Sci.* **1986**, *7* (C), 186−191.

(8) Dimou, A.; Tsimihodimos, V.; Bairaktari, E. The Critical Role of the Branched Chain Amino Acids (BCAAs) Catabolism-Regulating Enzymes, Branched-Chain Aminotransferase (BCAT) and Branched-Chain α-Keto Acid Dehydrogenase (BCKD), in Human Pathophysiology. *Int. J. Mol. Sci.* **2022**, *23*, 4022.

(9) Neinast, M.; Murashige, D.; Arany, Z. Branched Chain Amino Acids. *Annu. Rev. Physiol.* **2019**, *81*, 139−164.

(10) Von Holt, C.; Chang, J.; Von Holt, M.; Böhm, H. Metabolism and Metabolic Effects of Hypoglycin. *Biochim. Biophys. Acta* **1964**, *90*, 611−613.

(11) Westermann, C. M.; Dorland, L.; van Diggelen, O. P.; Schoonderwoerd, K.; Bierau, J.; Waterham, H. R.; van der Kolk, J. H. Decreased Oxidative Phosphorylation and PGAM Deficiency in Horses Suffering from Atypical Myopathy Associated with Acquired MADD. *Mol. Genet. Metab.* **2011**, *104* (3), 273−278.

(12) Lemieux, H.; Boemer, F.; van Galen, G.; Serteyn, D.; Amory, H.; Baise, E.; Cassart, D.; van Loon, G.; Marcillaud-Pitel, C.; Votion, D. M. Mitochondrial Function Is Altered in Horse Atypical Myopathy. *Mitochondrion* **2016**, *30*, 35−41.

(13) Cassart, D.; Baise, E.; Cherel, Y.; Delguste, C.; Antoine, N.; Votion, D.; Amory, H.; Rollin, F.; Linden, A.; Coignoul, F.; Desmecht, D. Morphological Alterations in Oxidative Muscles and Mitochondrial Structure Associated with Equine Atypical Myopathy. *Equine Vet. J.* **2007**, *39* (1), 26−32.

(14) Tanaka, K.; Miller, E. M.; Isselbacher, K. J. Hypoglycin A: A Specific Inhibitor of Isovaleryl CoA Dehydrogenase. *Proc. Natl. Acad. Sci. U.S.A.* **1971**, *68* (1), 20−24.
(15) Renaud, B.; François, A.-C.; Boemer, F.; Kruse, C.; Stern, D.; Piot, A.; Petitjean, T.; Gustin, P.; Votion, D.-M. Grazing Mares on Pasture with Sycamore Maples: A Potential Threat to Suckling Foals and Food Safety through Milk Contamination. *Animals* **2021**, *11* (1), 87.
(16) Baise, E.; Habyarimana, J. A.; Amory, H.; Boemer, F.; Douny, C.; Gustin, P.; Marcillaud-Pitel, C.; Patarin, F.; Weber, M.; Votion, D.-M. Samaras and Seedlings of Acer Pseudoplatanus Are Potential Sources of Hypoglycin A Intoxication in Atypical Myopathy without Necessarily Inducing Clinical Signs. *Equine Vet. J.* **2016**, *48* (4), 414−417.
(17) Bochnia, M.; Ziegler, J.; Sander, J.; Uhlig, A.; Schaefer, S.; Vollstedt, S.; Glatter, M.; Abel, S.; Recknagel, S.; Schusser, G. F.; Wensch-Dorendorf, M.; Zeyner, A. Hypoglycin a Content in Blood and Urine Discriminates Horses with Atypical Myopathy from Clinically Normal Horses Grazing on the Same Pasture. *PLoS One* **2015**, *10* (9), No. e0136785.
(18) Renaud, B.; François, A.-C.; Boemer, F.; Macillaud-Pitel, C.; Gustin, P.; Votion, D.-M. Diagnostic and Prognostic Value of Hypoglycin A, Methylenecyclopropyl Acetic Acid-Carnitine and, Acylcarnitines Profile in Horses with Atypical Myopathy. In *Proceedings of the 6th FARAH-Day*; University of Liège: Belgium, 2019.
(19) van Galen, G.; Marcillaud Pitel, C.; Saegerman, C.; Patarin, F.; Amory, H.; Baily, J. D.; Cassart, D.; Gerber, V.; Hahn, C.; Harris, P.; Keen, J. A.; Kirschvink, N.; Lefere, L.; McGorum, B.; Muller, J. M. V.; Picavet, M. T. J. E.; Piercy, R. J.; Roscher, K.; Serteyn, D.; Unger, L.; van der Kolk, J. H.; van Loon, G.; Verwilghen, D.; Westermann, C. M.; Votion, D. M. European Outbreaks of Atypical Myopathy in Grazing Equids (2006−2009): Spatiotemporal Distribution, History and Clinical Features. *Equine Vet. J.* **2012**, *44* (5), 614−620.
(20) Brandt, K.; Hinrichs, U.; Glitz, F.; Landes, E.; Schulze, C.; Deegen, E.; Pohlenz, J.; Coenen, M. Atypische Myoglobinurie Der Weidepferde. *Pferdeheilkunde* **1997**, *13* (1), 27−34.
(21) van Galen, G.; Saegerman, C.; Marcillaud Pitel, C.; Patarin, F.; Amory, H.; Baily, J. D.; Cassart, D.; Gerber, V.; Hahn, C.; Harris, P.; Keen, J. A.; Kirschvink, N.; Lefere, L.; Mcgorum, B.; Muller, J. M. V.; Picavet, M. T. J. E.; Piercy, R. J.; Roscher, K.; Serteyn, D.; Unger, L.; van der Kolk, J. H.; van Loon, G.; Verwilghen, D.; Westermann, C. M.; Votion, D. M. European Outbreaks of Atypical Myopathy in Grazing Horses (2006−2009): Determination of Indicators for Risk and Prognostic Factors. *Equine Vet. J.* **2012**, *44* (5), 621−625.
(22) Fabius, L. S.; Westermann, C. M. Evidence-Based Therapy for Atypical Myopathy in Horses. *Equine Vet. Educ.* **2018**, *30*, 616−622.
(23) Zhang, Z.; Wu, S.; Stenoien, D. L.; Paša-Tolić, L. High-Throughput Proteomics. *Annu. Rev. Anal. Chem.* **2014**, *7*, 427−454.
(24) Chiaradia, E.; Miller, I. In Slow Pace towards the Proteome of Equine Body Fluids. *J. Proteomics* **2020**, *225* (April), 103880.
(25) Aslam, B.; Basit, M.; Nisar, M. A.; Khurshid, M.; Rasool, M. H. Proteomics: Technologies and Their Applications. *J. Chromatogr. Sci.* **2017**, *55* (2), 182−196.
(26) Votion, D.-M.; François, A.-C.; Kruse, C.; Renaud, B.; Farinelle, A.; Bouquieaux, M.-C.; Marcillaud-Pitel, C.; Gustin, P. Answers to the Frequently Asked Questions Regarding Horse Feeding and Management Practices to Reduce the Risk of Atypical Myopathy. *Animals* **2020**, *10* (2), 365.
(27) Boemer, F.; Deberg, M.; Schoos, R.; Baise, E.; Amory, H.; Gault, G.; Carlier, J.; Gaillard, Y.; Marcillaud-Pitel, C.; Votion, D. Quantification of hypoglycin A in serum using aTRAQ® assay. *J. Chromatogr. B* **2015**, *997*, 75−80.
(28) Votion, D.-M. Analysing Hypoglycin A, Methylenecyclopropyl-acetic Acid Conjugates and Acylcarnitines in Blood to Confirm the Diagnosis and Improve Our Understanding of Atypical Myopathy. *Equine Vet. Educ.* **2018**, *30* (1), 29−30.
(29) Valberg, S. J.; Sponseller, B. T.; Hegeman, A. D.; Earing, J.; Bender, J. B.; Martinson, K. L.; Patterson, S. E.; Sweetman, L. Seasonal Pasture Myopathy/Atypical Myopathy in North America Associated with Ingestion of Hypoglycin A within Seeds of the Box Elder Tree. *Equine Vet. J.* **2013**, *45* (4), 419−426.
(30) Wiśniewski, J. R.; Zougman, A.; Nagaraj, N.; Mann, M. Universal Sample Preparation Method for Proteome Analysis. *Nat. Methods* **2009**, *6* (5), 359−362.
(31) Meier, F.; Brunner, A.-D.; Koch, S.; Koch, H.; Lubeck, M.; Krause, M.; Goedecke, N.; Decker, J.; Kosinski, T.; Park, M. A.; Bache, N.; Hoerning, O.; Cox, J.; Räther, O.; Mann, M. Online Parallel Accumulation-Serial Fragmentation (PASEF) with a Novel Trapped Ion Mobility Mass Spectrometer. *Mol. Cell. Proteomics* **2018**, *17* (12), 2534−2545.
(32) Matzke, M. M.; Waters, K. M.; Metz, T. O.; Jacobs, J. M.; Sims, A. C.; Baric, R. S.; Pounds, J. G.; Webb-robertson, B. J. M. Improved Quality Control Processing of Peptide-Centric LC-MS Proteomics Data. *Bioinformatics* **2011**, *27* (20), 2866−2872.
(33) Stanfill, B. A.; Nakayasu, E. S.; Bramer, L. M.; Thompson, A. M.; Ansong, C. K.; Clauss, T. R.; Gritsenko, M. A.; Monroe, M. E.; Moore, R. J.; Orton, D. J.; Piehowski, P. D.; Schepmoes, A. A.; Smith, R. D.; Webb-Robertson, B.-J. M.; Metz, T. O. Quality Control Analysis in Real-Time (QC-ART): A Tool for Real-Time Quality Control Assessment of Mass Spectrometry-Based Proteomics Data. *Mol. Cell. Proteomics* **2018**, *17* (9), 1824−1836.
(34) Lin, H.; He, L.; Ma, B. A Combinatorial Approach to the Peptide Feature Matching Problem for Label-Free Quantification. *Bioinformatics* **2013**, *29* (14), 1768−1775.
(35) Thomas, P. D.; Ebert, D.; Muruganujan, A.; Mushayahama, T.; Albou, L. P.; Mi, H. PANTHER: Making Genome-Scale Phylogenetics Accessible to All. *Protein Sci.* **2022**, *31* (1), 8−22.
(36) Kanehisa, M.; Furumichi, M.; Tanabe, M.; Sato, Y.; Morishima, K. KEGG: New Perspectives on Genomes, Pathways, Diseases and Drugs. *Nucleic Acids Res.* **2017**, *45* (D1), D353−D361.
(37) Kanehisa, M.; Furumichi, M.; Sato, Y.; Kawashima, M.; Ishiguro-Watanabe, M. KEGG for Taxonomy-Based Analysis of Pathways and Genomes. *Nucleic Acids Res.* **2023**, *51* (D1), D587−D592.
(38) Votion, D. M.; Linden, A.; Delguste, C.; Amory, H.; Thiry, E.; Engels, P.; van Galen, G.; Navet, R.; Sluse, F.; Serteyn, D.; Saegerman, C. Atypical Myopathy in Grazing Horses: A First Exploratory Data Analysis. *Vet. J.* **2009**, *180* (1), 77−87.
(39) Schober, P.; Boer, C.; Schwarte, L. A. Correlation Coefficients: Appropriate Use and Interpretation. *Anesth. Analg.* **2018**, *126* (5), 1763−1768.
(40) PeaksTeam. *PEAKS X User Manual*; Bioinformatics Solutions Inc., 2018, p 243.
(41) Qu, J.; Ko, C. W.; Tso, P.; Bhargava, A. Apolipoprotein A-IV: A Multifunctional Protein Involved in Protection against Atherosclerosis and Diabetes. *Cells* **2019**, *8* (4), 319.
(42) Yamamoto, K.; Fukuda, N.; Fukui, M.; Kai, Y.; Ikeda, H.; Sakai, T. Increased Secretion of Triglyceride and Cholesterol Following Inhibition of Long-Chain Fatty Acid Oxidation in Rat Liver. *Ann. Nutr. Metab.* **1996**, *40* (3), 157−164.
(43) Ge, S. X.; Jung, D.; Yao, R. ShinyGO: A Graphical Gene-Set Enrichment Tool for Animals and Plants. *Bioinformatics* **2020**, *36* (8), 2628−2629.
(44) Delguste, C.; Cassart, D.; Baise, E.; Linden, A.; Schwarzwald, C.; Feige, K.; Sandersen, C.; Rollin, F.; Amory, H. Myopathies Atypiques Chez Les Chevaux Au Pré: Une Série de Cas En Belgique. *Ann. Med. Vet.* **2002**, *146* (4), 231−243.
(45) Votion, D.-M.; Linden, A.; Saegerman, C.; Engels, P.; Erpicum, M.; Thiry, E.; Delguste, C.; Rouxhet, S.; Demoulin, V.; Navet, R.; Sluse, F.; Serteyn, D.; van Galen, G.; Amory, H. History and Clinical Features of Atypical Myopathy in Horses in Belgium (2000−2005). *J. Vet. Intern. Med.* **2007**, *21* (6), 1380.
(46) Boemer, F.; Detilleux, J.; Cello, C.; Amory, H.; Marcillaud-Pitel, C.; Richard, E.; van Galen, G.; van Loon, G.; Lefère, L.; Votion, D.-M. Acylcarnitines Profile Best Predicts Survival in Horses with At Myopathy. *PLoS One* **2017**, *12* (8), No. e0182761.
(47) Mathis, D.; Sass, J. O.; Graubner, C.; Schoster, A. Diagnosis of Atypical Myopathy Based on Organic Acid and Acylcarnitine Profiles

https://doi.org/10.1021/acsomega.3c06647
ACS Omega XXXX, XXX, XXX−XXX

and Evolution of Biomarkers in Surviving Horses. *Mol. Genet. Metab. Rep.* **2021**, *29*, 100827.
(48) Harrison, M. F. The Misunderstood Coagulopathy of Liver Disease: A Review for the Acute Setting. *West. J. Emerg. Med.* **2018**, *19* (5), 863−871.
(49) Mammen, E. F. Coagulation Abnormalities in Liver Disease. *Hematol./Oncol. Clin. North Am.* **1992**, *6* (6), 1247−1257.
(50) Holeček, M. Branched-Chain Amino Acids in Health and Disease: Metabolism, Alterations in Blood Plasma, and as Supplements. *Nutr. Metab. (London)* **2018**, *15* (1), 33.
(51) Giannoglou, G. D.; Chatzizisis, Y. S.; Misirli, G. The Syndrome of Rhabdomyolysis: Pathophysiology and Diagnosis. *Eur. J. Intern. Med.* **2007**, *18*, 90−100.
(52) Wrogemann, K.; Pena, S. D. J. Mitochondrial Calcium Overload : A General Mechanism for Cell-Necrosis in Muscle Diseases. *Lancet* **1976**, *307* (7961), 672−674.
(53) Rizzuto, R.; Pinton, P.; Ferrari, D.; Chami, M.; Szabadkai, G.; Magalhães, P. J.; Virgilio, F. D.; Pozzan, T. Calcium and Apoptosis: Facts and Hypotheses. *Oncogene* **2003**, *22*, 8619−8627.
(54) Zamzami, N.; Hirsch, T.; Dallaporta, B.; Petit, P. X.; Kroemer, G. Mitochondrial Implication in Accidental and Programmed Cell Death: Apoptosis and Necrosis. *J. Bioenerg. Biomembr.* **1997**, *29* (2), 185−193.
(55) Brookes, P. S.; Yoon, Y.; Robotham, J. L.; Anders, M. W.; Sheu, S.-S. Calcium, ATP, and ROS: A Mitochondrial Love-Hate Triangle. *Am. J. Physiol.-Cell Physiol.* **2004**, *287*, C817−C833.
(56) Poels, P. J. E.; Gabreels, F. J. M. Rhabdomyolysis: A Review of the Literature. *Clin. Neurol. Neurosurg.* **1993**, *95*, 175−192.
(57) Löfberg, M. Myosin Heavy-Chain Fragments and Cardiac Troponins in the Serum in Rhabdomyolysis. *Arch. Neurol.* **1995**, *52* (12), 1210.
(58) Barrey, E.; Mucher, E.; Jeansoule, N.; Larcher, T.; Guigand, L.; Herszberg, B.; Chaffaux, S.; Guérin, G.; Mata, X.; Benech, P.; Canale, M.; Alibert, O.; Maltere, P.; Gidrol, X. Gene Expression Profiling in Equine Polysaccharide Storage Myopathy Revealed Inflammation, Glycogenesis Inhibition, Hypoxia and Mitochondrial Dysfunctions. *BMC Vet. Res.* **2009**, *5* (1), 29.
(59) Valberg, S. J.; Perumbakkam, S.; McKenzie, E. C.; Finno, C. J. Proteome and Transcriptome Profiling of Equine Myofibrillar Myopathy Identifies Diminished Peroxiredoxin 6 and Altered Cysteine Metabolic Pathways. *Physiol. Genomics* **2018**, *50* (12), 1036−1050.
(60) Finno, C. J.; Valberg, S. J.; Wünschmann, A.; Murphy, M. J. Seasonal Pasture Myopathy in Horses in the Midwestern United States: 14 Cases (1998−2005). *J. Am. Vet. Med. Assoc.* **2006**, *229* (7), 1134−1141.
(61) Mohammed, H. O.; Divers, T. J.; Kwak, J.; Omar, A. H.; White, M. E.; de Lahunta, A. Association of Oxidative Stress with Motor Neuron Disease in Horses. *Am. J. Vet. Res.* **2012**, *73* (12), 1957−1962.
(62) de la Rúa-Domènech, R.; Wiedmann, M.; Mohammed, H. O.; Cummings, J. F.; Divers, T. J.; Batt, C. A. Equine Motor Neuron Disease Is Not Linked to Cu/Zn Superoxide Dismutase Mutations: Sequence Analysis of the Equine Cu/Zn Superoxide Dismutase CDNA. *Gene* **1996**, *178* (1−2), 83−88.
(63) Armstrong, R. N. Glutathione Transferases. *Compr. Toxicol.* **2010**, *4*, 295−321.
(64) Gumulec, J.; Raudenska, M.; Hlavna, M.; Stracina, T.; Sztalmachova, M.; Tanhauserova, V.; Pacal, L.; Ruttkay-Nedecky, B.; Sochor, J.; Zitka, O.; Babula, P.; Adam, V.; Kizek, R.; Novakova, M.; Masarik, M. Determination of Oxidative Stress and Activities of Antioxidant Enzymes in Guinea Pigs Treated with Haloperidol. *Exp. Ther. Med.* **2013**, *5* (2), 479−484.
(65) Huang, J.; Tan, P. H.; Tan, B. K. H.; Bay, B. H. GST-Pi Expression Correlates with Oxidative Stress and Apoptosis in Breast Cancer. *Oncol. Rep.* **2004**, *12* (4), 921−925.
(66) Tew, K. D.; Townsend, D. M. Glutathione-S-Transferases as Determinants of Cell Survival and Death. *Antioxid. Redox Signaling* **2012**, *17* (12), 1728−1737.
(67) Barrey, E.; Jayr, L.; Mucher, E.; Gospodnetic, S.; Joly, F.; Benech, P.; Alibert, O.; Gidrol, X.; Mata, X.; Vaiman, A.; Guérin, G. Transcriptome Analysis of Muscle in Horses Suffering from Recurrent Exertional Rhabdomyolysis Revealed Energetic Pathway Alterations and Disruption in the Cytosolic Calcium Regulation. *Anim. Genet.* **2012**, *43* (3), 271−281.
(68) Singer, E.; Markó, L.; Paragas, N.; Barasch, J.; Dragun, D.; Müller, D. N.; Budde, K.; Schmidt-Ott, K. M. Neutrophil Gelatinase-Associated Lipocalin: Pathophysiology and Clinical Applications. *Acta Physiol.* **2013**, *207*, 663−672.
(69) Wasung, M. E.; Chawla, L. S.; Madero, M. Biomarkers of Renal Function, Which and When? *Clin. Chim. Acta* **2015**, *438*, 350−357.
(70) Wouters, C. Metabolomic/Lipidomic Investigations in Equine Atypical Myopathy and in Vitro Screening of Non-Pharmaceutical Compounds, Université de Liège, 2021.
(71) Dunnett, M.; Harris, R. C.; Sewell, D. A. Taurine Content and Distribution in Equine Skeletal Muscle. *Scand. J. Clin. Lab. Invest.* **1992**, *52* (7), 725−730.
(72) Valberg, S.; Häggendal, J.; Lindholm, A. Blood Chemistry and Skeletal Muscle Metabolic Responses to Exercise in Horses with Recurrent Exertional Rhabdomyolysis. *Equine Vet. J.* **1993**, *25* (1), 17−22.
(73) Holloszy, J. O.; Constable, S. H.; Young, D. A. Activation of Glucose Transport in Muscle by Exercise. *Diabetes/Metab. Rev.* **1986**, *1* (4), 409−423.
(74) Lacombe, V. A.; Hinchcliff, K. W.; Kohn, C. W.; Devor, S. T.; Taylor, L. E. Effects of feeding meals with various soluble-carbohydrate content on muscle glycogen synthesis after exercise in horses. *Am. J. Vet. Res.* **2004**, *65*, 916−923.
(75) Jose-Cunilleras, E.; Hayes, K. A.; Toribio, R. E.; Mathes, L. E.; Hinchcliff, K. W. Expression of Equine Glucose Transporter Type 4 in Skeletal Muscle after Glycogen-Depleting Exercise. *Am. J. Vet. Res.* **2005**, *66* (3), 379−385.
(76) Huang, C. K.; Sun, Y.; Lv, L.; Ping, Y. ENO1 and Cancer. *Mol. Ther.–Oncolytics* **2022**, *24*, 288−298.
(77) Khan, F. Y. Rhabdomyolysis: A Review of the Literature. *Neth. J. Med.* **2009**, *67* (9), 272−283.
(78) Akmal, M.; Massry, S. G. Reversible Hepatic Dysfunction Associated with Rhabdomyolysis. *Am. J. Nephrol.* **1990**, *10* (1), 49−52.
(79) García-Cañaveras, J. C.; Peris-Díaz, M. D.; Alcoriza-Balaguer, M. I.; Cerdán-Calero, M.; Donato, M. T.; Lahoz, A. A Lipidomic Cell-Based Assay for Studying Drug-Induced Phospholipidosis and Steatosis. *Electrophoresis* **2017**, *38* (18), 2331−2340.
(80) Teresa Donato, M.; Jose Gomez-Lechon, M. Drug-Induced Liver Steatosis and Phospholipidosis: Cell-Based Assays for Early Screening of Drug Candidates. *Curr. Drug Metab.* **2012**, *13* (8), 1160−1173.
(81) Muto-fujita, A. A Novel Model for the Chemical Evolution of Metabolic Networks. *Bull. Chem. Soc. Jpn. B Chem. Soc. Jpn.* **2019**, *37* (3), 57−62.
(82) Valberg, S. J.; Velez-Irizarry, D.; Williams, Z. J.; Henry, M. L.; Iglewski, H.; Herrick, K.; Fenger, C. Enriched Pathways of Calcium Regulation, Cellular/Oxidative Stress, Inflammation, and Cell Proliferation Characterize Gluteal Muscle of Standardbred Horses between Episodes of Recurrent Exertional Rhabdomyolysis. *Genes (Basel)* **2022**, *13* (10), 1853.
(83) Avellini, L.; Chiaradia, E.; Gaiti, A. Effect of Exercise Training, Selenium and Vitamin E on Some Free Radical Scavengers in Horses (Equus Caballus). *Comp. Biochem. Physiol., Part B: Biochem. Mol. Biol.* **1999**, *123*, 147−154.
(84) Gomez, D. E.; Valberg, S. J.; Magdesian, K. G.; Hanna, P. E.; Lofstedt, J. Acquired Multiple Acyl-CoA Dehydrogenase Deficiency and Marked Selenium Deficiency Causing Severe Rhabdomyolysis in a Horse. *Can. Vet. J.* **2015**, *56* (11), 1166−1171.
(85) Koves, T. R.; Ussher, J. R.; Noland, R. C.; Slentz, D.; Mosedale, M.; Ilkayeva, O.; Bain, J.; Stevens, R.; Dyck, J. R. B.; Newgard, C. B.; Lopaschuk, G. D.; Muoio, D. M. Mitochondrial Overload and Incomplete Fatty Acid Oxidation Contribute to Skeletal Muscle Insulin Resistance. *Cell Metab.* **2008**, *7* (1), 45−56.

https://doi.org/10.1021/acsomega.3c06647
ACS Omega XXXX, XXX, XXX−XXX